A Complexity and Networks approach to Sustainability.

Nicky Zachariou

Department of Physics
and
Centre for Complexity Science

Imperial College London

This thesis is submitted in part fulfilment of the requirements of the degree of Doctor of Philosophy in Physics of Imperial College London and the Diploma of Imperial College London.

July 2016

Copyright

The copyright of this thesis rests with the author and is made available under a Creative Commons Attribution Non-Commercial No Derivatives licence. Researchers are free to copy, distribute or transmit the thesis on the condition that they attribute it, that they do not use it for commercial purposes and that they do not alter, transform or build upon it. For any reuse or redistribution, researchers must make clear to others the licence terms of this work.

Στην Αυγή, Ελένη και Ροβινσών.

My earth, wind and fire.

Declaration

I hereby declare that except where specific reference is made to the work of others, the contents of this dissertation are original and have not been submitted in whole or in part for consideration for any other degree or qualification in this, or any other University. Parts of this dissertation that have been published in peer reviewed journals have been clearly indicated as such in the text.

Nicky Zachariou

July 2016

Acknowledgements

As I was writing this I realised two things: one, that I am an extremely lucky person who is surrounded by very kind and good people and two, that I actually enjoyed this adventure and lived to tell the tale. I call this my *Seven Year Itch*. And below is the list of people that helped me grow up slightly and/or made my days better and/or helped shape my future whilst being extremely patient with me until I got there. They are all great friends and have taught me important lessons about life[1].

Thank you μάμα μου – for everything. If I am here today, it's because of you. You made the right decisions at the right time, regardless of personal cost and sacrifice and you have worked extremely hard so that I wouldn't need to. But most of all, thank you for passing onto me your love for education and your fierce energy for life.

Thank you παπά μου – for teaching me cards that taught me maths, for not taking 95 when you thought 100 was possible and for dancing with me, protecting me, being proud of me and supporting me until your final breath.

[1] If I have forgotten anyone it is because I am an awful person and I do not deserve your love and forgiveness. I am truly sorry.

Thank you μάμα θεία Ελένη μου – for being my second mum and my best friend and for asking me at age two what I was going to be when I grow up and for patiently waiting for the answer still.

Thank you Kim – for persistently fighting for me and holding my hand through all the hurdles, for knowing what to do when everything was taken away. But most importantly thank you for being my teacher and a great friend. I will be forever in your debt.

Thank you Henrik – for not giving up on me, for giving me enough freedom to find myself but subtly guiding me along the way and inspiring me to be an all rounded mathematician.

Thank you Paul – for taking me under your wing, for being a great friend and companion in this journey, for being stuck in the toilet during the 311 earthquake, for knowing the Japanese words for explosion and alcohol and finally for teaching me what a real scientist is and helping me realise that I am not one.

Thank you Gunnar – for making me realise that (a) *this is real life, I can just open the door and get out of here* and (b) *who cares about all that I know, it's what I don't that's exciting!*

Thank you Shama and Kishan – for pushing the boundaries and helping me spread the word on complexity and networks to non-scientists.

Thank you Rishi – for using data for good and for making a full time job and a weekend PhD an attractive idea. It was tough, but I made it and you will too.

Thank you Fatimah – for praying for me and for shuttering all the stereotypes.

Thank you Misako – for welcoming me to Japan with open arms, but most importantly for not succumbing to gender biases and showing me first hand that when sexist people serve you lemons you don't just make lemonade, you raise capital and buy the equivalent dataset from their competitors.

Thank you Hideki – for showing me that interesting research can be done both within and outside of academia and that to succeed I always need to be ahead of the curve.

Thank you Wataru, Hayafumi, Yura, Yukie and Taro – for introducing me to many new experiences, be it raw chicken or cooked oysters. Also, thank you Yura – for showing me that it is important to do what you are passionate about regardless of the personal costs.

Thank you Adrian – for taking charge and succeeding in getting Paul and I safely home by *any* means necessary, because hindsight is a luxury that arrives a minute too late.

Thank you Maria – for making sandcastles, playing mermaids, being a lady and making the days that I see you absolutely spectacular.

Thank you Elena – for still sending me handwritten letters by post, for showing me that "you only fail when you stop trying" and finally for succeeding against all odds.

Thank you Giovanna – for choosing all the flavours of ice cream, for creating databeers just for fun and for sending me two copies of *The Thirtieth Year* when I was in my late twenties because you thought I needed to read it and would appreciate a head start.

Thank you Peter – for being my favourite brother, a stable tree with deep roots.

Thank you kids – Alex for your endless wisdom and thirst for knowledge. Dylan for counting in batches of sixteen and for not touching my laptop during simulations, even though you really wanted to. Melissa for approaching every situation with a smile first.

Thank you Timon – for picking up the phone on that day, for being a constant positive influence ever since and for falling multiple times but still getting up to finish the dance.

Thank you Ιάκωβε – for the music and the lyrics.

Thank you Μάριε – for showing me that it's possible to find out what you want to be when you grow up and then do everything in your power to be it.

Thank you Dean – for perfecting my right hook, for kicking the pedestal and for making me feel like anything is physically possible.

Thank you Gauss – for being the best dog and for keeping me company all these sleepless nights that I stayed up writing this thesis.

Thank you Τόπη μου – for not giving up when I did and for being a grown up and a kid.

Κάντε υπομονή, κι ο ουρανός θα γίνει πιο γαλανός.
Κάντε υπομονή, μια λεμονιά ανθίζει στη γειτωνιά.

Αλέκος Σακελλάριος[2]

[2]Translation: Be patient, and the sky will become more blue. Be patient and a lemon tree is blooming in the neighborhood.

Abstract

Sustainability is a key issue of the 21st century. A complexity and networks approach is taken to investigate what makes socio-economic systems sustainable, or not, and what lessons that can be learned from the sandpile model, an analogy of observed economic activity.

The sandpile model has been studied extensively on regular lattices with fixed coordination number $K = 2$. Here, the dynamics is generalised to evolve on less rigid networks. The regular lattice structure is relaxed by introducing an inter-layer distribution for the interactions between nodes. This forces the scaling exponent of the avalanche-size probability density function out of the two-dimensional directed sandpile universality class $\tau = 4/3$, into the mean field universality class $\tau = 3/2$.

An apparent drift in the exponents of the avalanches found in the Monte Carlo simulations on a lattice with $K > 2$ is attributed to the observed holes and side-branches of avalanche clusters, which leads to large corrections to scaling. The $K = 3$ case is solved analytically, proving that in fact the critical exponents for $K > 2$ are identical to the $K = 2$ case.

The most realistic topology that can be used to model economic activity is the production-

consumption network between firms in a real economy. A novel avalanche-size exponent $\tau \approx 1.87$, that falls outside the two known universality classes, emerges when the model evolves on the Japanese inter-firm network. This network has the typical bow-tie structure of a real-world directed network: in and out-layers, and a strongly connected component. The strongly connected component is not layered and displays a large range of network motifs [61].

Randomly adding a small proportion of links between non-adjacent layers in one of the layered networks in the mean-field universality class, abruptly takes the system out of the mean-field regime with a non-trivial avalanche-size probability density function, which closely reproduces the behaviour observed on the real-world Japanese network.

Contents

Contents **13**

List of Figures **17**

List of Tables **25**

Nomenclature **27**

1 Introduction **29**

1.1 Motivation 29

1.2 Thesis Outline 30

1.3 List of Publications 33

2 Sustainability **35**

2.1 The world we live in 35

2.2 The principles of Sustainability 38

2.3 Thinking in systems 40

2.4 Seeking Sustainability in an age of complexity 42

2.5 Summary 44

3 Complexity and Networks **47**

3.1 Reductionism Limitations 47

3.2 Complexity Science 49

3.2.1 Insect Colonies 50

3.2.2 Economies 51

3.2.3 The Earth 52

3.3 Adaptability of Complex Systems 53

3.4 Emergence 54

3.5 Network Science 54

3.6 Summary 58

4 The generalised sandpile model as a paradigm for economic activity **61**

4.1 Introduction 61

4.2 Model definition of the generalised sandpile 66

4.3 Theoretical framework 71

4.4 Results on a regular lattice with $K \geq 2$ 73

4.5 Summary 77

5 Analytical solution of the directed sandpile model for $K \geq 2$ 79

5.1 Introduction . . . 79

5.2 Model definition . . . 81

5.3 Calculation of the 2-point correlation function . . . 84

5.4 Calculation of the 3-point correlation function . . . 88

5.5 Corrections to scaling . . . 99

5.6 Numerical simulations . . . 102

5.6.1 Initialisation . . . 102

5.6.2 Parameters and Results . . . 103

5.7 Summary . . . 109

6 Avalanches in the real-world inter-firm network of the Japanese economy 111

6.1 Introduction . . . 111

6.2 Methods . . . 114

6.3 Results on less rigid networks . . . 115

6.3.1 Japanese inter-firm network . . . 116

6.3.2 Layered lattice with inter-layer distribution of interactions . . . 118

6.3.3 Long range connections across layers . . . 123

6.4 Summary . . . 126

7 Discussion **129**

7.1 Conclusions 129

7.2 Outlook 132

Bibliography **135**

List of Figures

3.1 **Network of acknowledgements.** The social network of the individuals in the acknowledgements section, where nodes are numbered in order of appearance in the text and coloured according to whether they are family (red), academics (grey) and close friends (blue). The average path length is 1.86 and the average degree is 9.3. Node 6 is a hub node, as it is connected to 70% of the other nodes in the network and its degree (22), greatly exceeds the average. It also has the highest betweenness centrality (166), which means that it acts as the predominant bridge along the shortest path between most pairs of nodes. 56

4.1 **Illustration of a sandpile in bureaucracy.** Bureaucrats remain inactive until four or more pieces of paper requiring action are found on their desk, at which point they will send one piece of paper to each of their nearest neighbours. After some time, the system will reach a point where a single piece of paper entering the office will cause an avalanche of papers being shuffled around. This light-hearted application of the sandpile to a bureaucratic setting is courtesy of the physicist Peter Grassberger who, ironically, is famous for his research in chaos theory. 64

4.2 **Illustration of regular lattice topologies.** Networks shown are subsets of: (a) a two-dimensional directed lattice with coordination number $K = 2$; (b) a two-dimensional directed lattice with coordination number $K = 4$. Periodic boundary conditions are applied to the left- and right-most nodes to form a cylindrical structure. The nodes in the top layer are the final goods producers, the nodes in the bottom layer are providers of raw materials and all other nodes between are the producers of intermediate goods. It is left to the readers imagination to extend this setup to higher co-ordination numbers $K > 4$. 67

4.3 **Illustration of a local process with and without production.** Networks shown are subsets of a two-dimensional directed lattice with coordination number $K = 2$ with different initial inventory configurations: (a) the producer node (black) receives an order from its customer, the activated (red) node in the layer above, and since it can fulfil the order from the product in its inventory it will simply hand it over and not go into production, $y_{i,j}(t) = 0$, resulting in an empty inventory in the final configuration; (b) the producer node (black) receives two orders from both its customer, the activated (red) nodes in the layer above, and since this time it cannot fulfil both orders from the product in its inventory it must produce to its full capacity, $y_{i,j}(t) = k^{in}_{i,j}$ which is 2 units in this case, and give the product to its customers leaving all inventories full in the final configuration. 69

4.4 **Results on regular lattice with higher coordination number.** The main figure shows the data collapse for different coordination numbers K of the avalanche-size pdfs $P(y;L)$ obtained by plotting the transformed avalanche-size pdf $y^{\tau}P(y;L)$ against the rescaled avalanche size y/L^{D} using the estimates of the avalanche-size scaling exponents τ and D obtained from moment scaling analysis, see Table 4.1. The line style indicates the system size, dotted line: $L = 200$; dashed line: $L = 400$; solid line: $L = 600$. The width of the system is kept constant at $M = 2000$ nodes. The colours show the coordination number for the regular lattice underlying networks; $K = 2$ (grey), $K = 4$ (red), $K = 6$ (blue), $K = 8$ (black). The inset displays the avalanche-size pdf $P(y;L)$ plotted against the avalanche size y after logarithmic binning was used. 75

5.1 **Illustrations of avalanches.** Three randomly selected examples of avalanches for systems with co-ordination numbers $K = 2$ (top row) and $K = 3$ (bottom row), with avalanche sizes $s = 201; 406; 802$ and $s = 201; 404; 805$ respectively. The avalanches start at the top row ($t = 0$) and for display purposes have been centred around their seed node. The lattices used to generate these results have height $L = 64$ and width $M = 160$; only the middle 64 columns are displayed here as these are enough to show the trajectory of the avalanche. The toppled sites have an off-white colour and the remaining sites have different shades of brown based on their height at the end, when the avalanche has stopped. For $K = 2$ the allowed heights are $h(x,t) = 0, 1$ and for $K = 3$ a site does not topple for $h(x,t) = 0, 1, 2$. The avalanches for $K = 2$ are compact as opposed to the avalanches for $K = 3$. Also, notice the $K = 3$ avalanches can have side branches. 81

5.2 **Illustration of the directed sandpile model on a cylindrical lattice.** Each site has $K = 3$ downward neighbours and is allowed to have a height of $h(x,t) = 0, 1, 2$, where $t = 0, 1, ..., L-1$ and $x = 0, 1, ..., M-1$. When the height exceeds 2, then the site is said to topple and one particle is transferred to each of its $K = 3$ downward neighbours as denoted by the arrows. The light cone of the top site, the seed node, is indicated with sites having black circles; sites in grey will be unaffected by any avalanche initiated at that specific seed. 82

5.3 **Corrections to scaling.** The main figure shows the behavior of the mean squared flux $\langle \Phi^2(t) \rangle$ as a function of the depth t, $1 \leq t \leq 1000$, determined from the exact series expansion of $\tilde{F}(z)$ (black dotted line) in a double-logarithmic plot. The best visual fit to the function $f(t) = at^{\alpha}$ given by the estimated parameters $a \approx 1.61, \alpha \approx 0.52$ (grey dashed line). In the inset, we plot effective exponent α_t, defined in Eq. (5.47) (black dotted line) which slowly converges to the exact value 0.5 (grey dashed line), as $\langle \Phi^2(t) \rangle \propto t^{1/2}$. Both plots in this figure show that corrections to scaling are still large for avalanches of duration of order 10^3, that is, avalanches that reach $t = 1000$. 100

5.4 **Moments analysis.** The scaled moments $\langle s^n \rangle L^{-\mu_n}$ plotted against the height of the lattice L for $n = 2, 3, 4, 5$. The data shown is for different $K = 2$ (red circles), $K = 3$ (green squares) and $K = 4$ (blue diamonds). For the same K, a higher curve corresponds to higher n. Note that for increasing K, the corrections to scaling become more important. 104

6.1 **Results on the Japanese inter-firm network.** The avalanche-size pdf $P(y)$ versus the avalanche size y obtained when the directed generalised dynamics evolves on the inter-firm network (solid black line). For more than three orders of magnitude, this pdf is well approximated with a power-law decay $P(y) \propto y^{-1.87}$, for $20 \lesssim y \lesssim 30000$. The grey dashed lines with $\tau = 4/3$ and $\tau = 3/2$ are guides to the eyes for the known universality classes' avalanche-size exponents of directed ($d = 2$) and mean-field, respectively. 118

6.2 **Results on lattices with Gaussian out- and in-degree inter-layer distributions.** The main figure shows the data collapse of the avalanche-size pdfs $P(y;L)$ from networks with underlying Gaussian out-degree distribution, obtained by plotting the transformed avalanche-size pdf $y^{\tau}P(y;L)$ against the rescaled avalanche size y/L^{D} using the estimates of the avalanche-size scaling exponents τ and D obtained from moment scaling analysis, see Table 6.1, L=200 (dashed-dotted); L=400 (dashed line); L=600 (solid line). The line colour indicates the standard deviation: $\sigma = 0$ (red), $\sigma = 1$ (blue), $\sigma = 2$ (black). By CLT the in-degree is also Gaussian distributed. The width of the system is $M = 2000$ nodes. The inset displays the avalanche-size pdf $P(y;L)$ versus the avalanche size y. 120

6.3 **Results on lattices with scale-free out- and Gaussian in-degree inter-layer distributions.** The main figure shows the data collapse of the avalanche-size pdfs $P(y;L)$ from networks with underlying truncated scale-free out-degree distribution and, by Central Limit Theorem (CLT), Gaussian in-degree distribution. These were obtained by plotting the transformed avalanche-size pdf $y^{\tau}P(y;L)$ against the rescaled avalanche size y/L^{D} using the estimates of the avalanche-size scaling exponents τ and D obtained from moment scaling analysis, see Table 6.2. The line style indicates the system size, dashed-dotted: L=200; dashed line: L=400; solid line: L=600. The line colour indicates the scale-free exponent γ: $\gamma = 2.5$ (red), $\gamma = 3.0$ (blue), $\gamma = 3.5$ (black). The width of the system is kept constant at 2000 nodes. The inset displays the avalanche-size pdf $P(y;L)$ plotted against the avalanche size y generated from networks with underlying truncated scale-free out-degree distribution. 121

6.4 **Results on lattices with scale-free in- and out-degree inter-layer distributions.** The main figure shows the data collapse of the avalanche-size pdfs $P(y;L)$ from networks with underlying truncated scale-free in- and out-degree distribution. These were obtained by plotting the transformed avalanche-size pdf $y^{\tau}P(y;L)$ against the rescaled avalanche size y/L^{D} using the estimates of the avalanche-size scaling exponents τ and D obtained from moment scaling analysis, see Table 6.3. The line style indicates the system size, dashed-dotted: L=100; dotted line: L=200; dashed line: L=400; solid line: L=600. The line colour indicates the scale-free exponent γ: $\gamma = 2.5$ (red) with $L = 100, 200, 400$ and $\gamma = 3.5$ (black) with $L = 200, 400, 600$. The width of the system is $M = 2000$ nodes. The inset displays the avalanche-size pdf $P(y;L)$ versus the avalanche size y. 123

6.5 **Illustration of the types of layered topologies tested.** Networks shown are subsets of (a) two-dimensional rigid regular directed lattice with co-ordination number $K = 2$ (black dashed lines); (b) layered network with a randomised inter-layer degree distribution (e.g. Gaussian or Scale-free) with randomly chosen neighbours in the adjacent layer below (black solid lines); (c) networks created by adding links connecting non adjacent layers (red solid lines) in both directions to the layered network with randomised degree distribution (black solid lines). In all cases, periodic boundary conditions are applied to the left- and right-most nodes to form a cylindrical structure. 124

6.6 **Results on lattices with long-range connections.** The avalanche-size pdf $P(y)$ versus the avalanche-size y obtained using the inter-firm Japanese network (solid black line). The dashed red line is the pdf $P(y)$ obtained with 25% of long range connections across layers in an otherwise layered network with nodes in- and out- degree drawn from a truncated scale-free distribution with exponent $\gamma = 2.5$ and system size $L = 400$. The grey dashed lines are guides to the eyes for the different avalanche-size exponents ($\tau = 4/3$ and $3/2$) of the known universality classes for the directed sandpile model and the approximate $\tau = 1.87$ that seems to fit the pdfs of inter-firm Japanese network. 126

List of Tables

4.1 **Scaling exponents on regular lattices.** The avalanche-size exponent, τ, and the avalanche-dimension, D, for regular lattice structures with coordination numbers, $K = 2, 4, 6, 8$ and circumference M, see Fig. 4.4 for the data collapse. The numbers in the brackets indicate the estimated errors of the exponents. The scaling relation $D(2-\tau) = 1$, see Eq. (4.11), is fulfilled (see last column) and, within error bars, both scaling exponents (apart from $K = 8$ and $M = 2000$) are consistent with the universality class of the two-dimensional directed sandpile model $\tau = 4/3$ and $D = 3/2$. The numerical result for $K = 8$, $M = 2000$ and 4000 suggests that the apparent drift is due to finite size effects. 76

5.1 **Scaling exponents on regular lattices with corrections to scaling.** Numerical estimates of the avalanche dimension D, and the avalanche-size exponent τ that was derived from it via the scaling relation $\tau = 2 - 1/D$. The numerics for $K = 2$ were performed as a reference, as $D = 3/2$ and hence $\tau = 4/3$ was already known analytically [26]. The first two columns are fits without including corrections to scaling. The last two columns list the exponents extracted when the fit includes corrections to scaling (ctos) Eq. (5.52) for systems with $K = 3$ and 4. The errorbars listed in the brackets correspond to three standard deviations of the last two significant digits. When corrections to scaling are taken into account, the data is consistent with $D = 3/2$ and $\tau = 4/3$ for all K considered. 107

6.1 **Scaling exponens on layered lattices with Gaussian out- and in-degree inter-layer distributions.** The avalanche-size exponent, τ, and the avalanche-dimension, D, for networks with nodes' out-degrees drawn from a Gaussian distribution with a fixed mean coordination number $\mu = 4$, and standard deviations $\sigma = 0, 1, 2$. Note that the case of $\sigma = 0$ is just a randomly rewired version of the regular lattice with coordination number $K = 4$, see Fig. 6.2 for the data collapse. The numbers in the brackets indicate the estimated errors of the exponents. Within error bars, both scaling exponents are consistent with the mean-field model $\tau = 3/2$ and $D = 2$. The last column shows that the exponents fulfill the scaling relation $D(2 - \tau) = 1$, see Eq. (4.11). 119

6.2 **Scaling exponents with scale-free out- and Gaussian in-degree inter-layer distributions.** The avalanche-size exponent τ and dimension D for networks with nodes' out-degrees drawn from a truncated scale free distribution with exponent $\gamma = 2.5, 3.0, 3.5$, see Fig. 6.3 for the data collapse. The CLT ensures the distribution of in-degrees is Gaussian. The estimated errors of the exponents are in the brackets. Within error bars, both scaling exponents are consistent with the mean-field model $\tau = 3/2$ and $D = 2$. The last column shows that the exponents fulfill the scaling relation $D(2-\tau) = 1$, see Eq. (4.11). 121

6.3 **Scaling exponents on layered lattices with scale-free in- and out-degree inter-layer distributions.**The avalanche-size exponent, τ, and the avalanche-dimension, D, for networks with nodes' in- and out-degrees were both drawn from a truncated scale free distribution with exponents $\gamma = 2.5, 3.5$, see Fig. 6.4 for the data collapse. The numbers in the brackets indicate the estimated errors of the exponents. Within error bars, both scaling exponents are consistent with the mean field-model $\tau = 3/2$ and $D = 2$. The last column shows that the exponents fulfill the scaling relation $D(2-\tau) = 1$, see Eq. (4.11). 122

Chapter 1

Introduction

1.1 Motivation

Complexity science deals with systems consisting of a large number of interacting components, whose aggregate activity cannot be predicted by the summation of the activity of the individual components alone [41]. One such complex system is the economy.

The economy of a country is made up of all the interactions within the country's inter-firm network. A long-standing problem in macroeconomic theory is explaining the unsustainable large fluctuations in aggregate economic activity that can result from many small, independent shocks to individual sectors [77]. It is of utmost importance as these can occur suddenly, cannot be effectively planned against and their effects can persist for a long time.

This behaviour is analogous to a model stemming from condensed matter theory, the sand-

pile model, a non-equilibrium system that self-organises into a critical scale-free state. Once settled at the steady state, the system has two characteristic timescales: at the slow timescale the system is driven by a grain of sand being added one at a time and at the fast timescale the system relaxes by a sudden burst of activity with a frequency-size distribution that is scale-free, with avalanches of all sizes and all durations [2]. Investigating how the dynamics of the generalised sandpile evolves on more realistic networks of the economy can shed some light on the causes of the large fluctuations.

The real-world inter-firm network of all active companies in the Japanese economy is a prime candidate for this study; the topology of this network is non-layered and directed, displaying the typical bow-tie structure found in real-world directed networks, with cycles and triangles. The emerging large fluctuations, that are observed when the generalised sandpile dynamics evolves on this network, can be detrimental to the sustainability of the system. It would be highly desirable if one could mitigate or even prevent them.

Understanding the mechanisms behind this example provide great insight as to what makes socio-economic systems sustainable.

1.2 Thesis Outline

The remainder of this thesis is arranged as follows.

In Chapter 2, the notion of sustainability is introduced and its importance in the world we currently live in is discussed in detail. Humans are seen as the dominant species and the sustainability of a human society is based mainly on the way the society is organised

rather than solely its relationship with the environment. Human societies have a lot to learn from the fundamental principles of governance in the systems of the natural world. Great insight can be drawn from modelling a human society as a complex system striving for its sustainability where the behaviour of the inter-connected socio-economic systems in the macroscale is really emerging from the interactions of the individuals in the microscale.

In Chapter 3, complex systems are explored. Complexity is an interdisciplinary field of research that tries to understand how large numbers of simple components self-organise, without the control of a central instructor, into a collective whole with macroscopic emerging coherent states that shares information and evolves. Colonies of social insects are introduced as some of the most mysterious and knowledge wealthy examples of complex systems in nature, whereas economies are a man made counterpart which are thought of being adaptive complex systems both on the micro- and macroscale. Social communities are networks made up of a large collection of nodes connected with edges; the nodes are the entities making up the social structure such as people, firms or insects whose many different types of relationships are characterised by the edges joining them. Thus, network science is proposed as a method of representing the complex systems under investigation.

In Chapter 4, the sandpile model is introduced and redefined as a model for studying behaviour in socio-economic systems. A more general form of the traditional dynamics is left to evolve on different regular network topologies with multiple neighbours per site. One can move from a strictly layered and rigid regular lattice, where the directed sandpile model has been studied until now, to a more flexible structure, by relaxing the regular lattice structure and introducing an interlayer distribution for the interactions. This forces the scaling exponent of the avalanche-size probability density function out of the two-dimensional directed sandpile universality class $\tau = 4/3$, into the mean field universality class $\tau = 3/2$.

In Chapter 5, it is shown both analytically and numerically that the generalisation of the directed sandpile model (see Chapter 4) on a square lattice, with K downward neighbours per site, where $K > 2$, is in the same universality class as $K = 2$ case which has previously been solved analytically. For $K > 2$, the avalanche clusters have side-branches that create holes into the otherwise compact avalanches obtained in the $K = 2$ case. Nevertheless, the large scale structure of the avalanches for $K > 2$ tends to the $K = 2$ case and yields the same critical exponents, which leads to the conclusion that the generalised sandpile model on a regular lattice is in the same universality class for all $K \geq 2$ [27].

In Chapter 6, avalanches in the economy are investigated when the generalised sandpile dynamics evolves on the real-world inter-firm network of all active companies in the Japanese economy. A novel avalanche-size exponent ($\tau \approx 1.87$ [98]) is observed, which does not fall into any of the two universality classes already discussed. Randomly adding a small proportion of links connecting non-adjacent layers, in an otherwise layered network with an interlayer distribution for the interactions, takes the system out of the mean field regime to produce a non-trivial avalanche-size probability density function that closely reproduces the behaviour observed on the Japanese inter-firm network.

Finally, the last chapter is a discussion which focuses on conclusions drawn from this research and plans for future work.

1.3 List of Publications

From Chapters 4 and 6

Zachariou, N., Expert, P., Takayasu, M., and Christensen, K. (2015). Generalised Sandpile Dynamics on Artificial and Real-World Directed Networks. *PLoS ONE,* 10(11):e0142685.

From Chapter 5

Dhar, D., Pruessner, G., Expert, P., Christensen, K., and Zachariou, N. (2016). Directed Abelian sandpile with multiple downward neighbors. Phys. Rev. E, **93**:042107.

Chapter 2

Sustainability

2.1 The world we live in

Our Earth is very different to Mars and Venus. As far as we have explored, it is the only planet with the unique property of sustaining itself and providing a nurturing environment for its living organisms [48, 78]. The debate as to whether this property of our planet is a result of its accidental position in our Solar System or is just a simple consequence of the life on its surface persists until the present day [48, 49]. Nevertheless, what remains is that, we, the dominant living things on this earth, should have a responsibility towards each other, to the other organisms and to Gaia herself to leave her behind in at least the same condition as we inherited her. The name Gaia stems from the Greek mythological goddess of the Earth, Γαία; James Lovelock revived this name in his 1979 controversial book *Gaia: A New Look at Life on Earth* [48], where he introduced his hypothesis: that all living organisms and inorganic material found on Earth are part of a tightly-coupled dynamic system that

self-regulates to maintain an environment fit for life.

The human species has always lived in an ever changing world over the past quarter of a million years. It not only suffered catastrophic events such as earthquakes, volcano eruptions and ice ages, but has also evolved physically, culturally and politically to adhere with its time. Our extraordinary progress in the last millennia has brought on an unrivalled level of advancement in the technological, economical, environmental and social domain [37]. As a result, population growth alone has made us the dominant species on Earth, with the power to alter the planet's natural course and cause irreparable damage to the ecosystem which houses us [95].

Over time, our basic instinct to protect ourselves against predators, pandemics and natural disasters has cemented the idea that we, the human species, must persevere by any means necessary. Added value was placed on the needs and desires of man, regardless of the consequences to the planet. What we overlooked in this endeavour is that our species is not isolated and in fact depends upon all the other organisms on Earth. Our survivability is interlinked with the survivability of all the other living things in our ecosystem and more importantly is coupled to the health of our planet [48].

Our advancement in technology, our rate of resource usage and our drive towards industrialisation has affected the planet in unprecedented measures. Luckily or not, depending on your point of view, our activities are approaching the limits provided by the global cycles of water, food and energy. Highly connected transportation and communication systems have enabled the diffusion of economic activity and with it the exploitation of about every inch of this Earth. Unfortunately, we single handedly bear the responsibility of being the "dominant planetary engineers" [37].

The past few decades have given us a glimpse into the detrimental effects of our new relationship with our ecosystem. The observed *global changes*[1] include, but are not limited to, desertification, deforestation, species extinction, atmospheric chemistry, climate change, water pollution, floods, drought, growing poverty and frequent epidemics [37, 95]. The causes of these are solely dependent upon the activities of the ever increasing number of people. The observed bursts of economic activity in the last two centuries, which were mainly due to technological development, caused unsustainable demands of energy and resource use [38]. The situation is extremely serious; the factors that cause these changes continue to advance at the same rate.

At the same time, we should not let our concerns over the irreparable changes we have caused cast a complete shadow over the many successes of the last millennium. Let us not forget that, before the advancements that brought us here, life was mostly short and difficult by the current Western standards. The United Nations Millennium Goals [86] were drafted in 2000 with the intention of providing a clear understanding of where we stand as a society and the outstanding problems we must address in the next millennium: the key two being sustainability and development. At first glance these may seem unrelated, but at close inspection one realises that you cannot have a success in one without the other; any progress made in development will not last unless it is made in a sustainable way. Ultimately, and due to our current way of making decisions, sustainability is at the mercy of the actions of individuals based on the information and the incentives they receive from governmental policies and the state of the economy at a local level, but also from the markets and other global interactions [37]. The behaviour of the inter-connected socio-economic systems in the macroscale is really determined by the interactions of the individuals in the microscale.

[1] Global changes occur on a planetary-scale in the Earth system, which includes the atmosphere, the land and the oceans, the natural cycles and all living organisms [81].

2.2 The principles of Sustainability

Sustainability as an idea has been gaining momentum in recent years. The word (un-) sustainable appears on governmental leaflets, the back of packaging and television adverts. We understand that it is an important idea, we must live our lives in a sustainable way, but most of us do not really understand what this exactly entails; sustainability is much more than being environmentally friendly, although caring for the environment is a good start.

In its modern form, sustainability as a concept was used as far back as 1974 by the World Council of Churches in their report to the ecumenical study conference [94]. It came as an answer to the world's developing countries, which had an objection to worrying about the environment, when other crucial matters such as poverty and deprivation of fundamental resources took precedence. The concept of a *sustainable society*, surprisingly, does not impose environmental conditions but instead imposes social conditions; it follows the principle of equatable distribution and democratic participation. Simply put, a sustainable society is one which will not self-destruct. Sustainability should just emerge at the crossroads between concerns for the global environment and global social justice. The difficulty then truly lies in reconciling the natural limits to growth with the concerns to social justice. The notion of sustainable development was introduced not long after [32].

In 1987, the United Nations World Commission on Environment and Development (WCED) published *Our Common Future* [11], a fundamental report highlighting the importance of sustainability and more so, of sustainable development. The *Brundtland Report*[2] as it became known, attempted to stress the importance of the intertwined relationship between economic development and environmental protection:

[2]Named after the Norwegian prime minister Gro Harlem Brundtland who chaired the UN General Assembly for World Commission on Environment and Development for the duration of its existence from 1983-1987.

"Through our deliberations and the testimony of people at the public hearings we held on five continents, all the commissioners came to focus on one central theme: many present development trends leave increasing numbers of people poor and vulnerable, while at the same time degrading the environment. How can such development serve next century's world of twice as many people relying on the same environment? This realization broadened our view of development. We came to see it not in its restricted context of economic growth in developing countries. We came to see that a new development path was required, one that sustained human progress not just in a few pieces for a few years, but for the entire planet into the distant future. Thus 'sustainable development' becomes a goal not just for the 'developing' nations, but for industrial ones as well [11, 28]."

The report proceeds to define sustainable development as one which *"meets the needs of the present without compromising the ability of future generations to meet their own needs."* They emphasised that the concept of sustainable development implies limits on environmental resources, which are placed by the current state of technological advancement and social organisation; the Earth cannot be stretched beyond her ability "to absorb the effects of human activities". However, both technology and social organisation are variables that can be explored and managed so as to pave the way to a more sustainable economic growth. The result of this should be a drastic reduction in poverty, where the basic needs of all are met. It is the belief of the Commission that a world without poverty is one which is less prone to environmental disasters and conversely, a world less prone to environmental disasters is one without poverty [11].

Finally, the Brundtland report acknowledges the difficulties in reaching this goal. It emphasises that sustainable development implies equity, both within and also between generations [28]. Moreover, sustainable development is not a fixed and stable state of peacefulness. In-

stead, it should be a growth process where the direction of technological development, the change in social organisation and the use of resources does not handicap the future generations whilst trying to meet our generation's needs.

The report served the purpose of formulating the issue and making imminent that our current destructive trends could not carry on with the everyday business as usual attitude. Difficult and unpopular choices needed to be made and it prompted governments and international agencies to seriously consider how to take action [85]. However, as with anything that rests on the shoulders of political will, the effect and results of any discussions were, and still are, very slow.

2.3 Thinking in systems

After the Brundtland report many international agreements have been prepared, signed, legalised and the resulting actions taken [85], the most notable being the Kyoto Protocol [87] that became legally binding in 2005 and all agreed parties committed to reduce their green house emissions according to internationally set targets. During the lengthy process of drafting these agreements, the governments of the countries involved have allocated parts of their budgets to programmes at the local and national levels with the aim of influencing people to make choices in the direction of a more sustainable future. However, many of the social and environmental indicators used for measuring the effect of humans on the biosphere continue to deteriorate: an additional 90 million people are pushed into poverty, 125 million are pushed into malnutrition to join the 1.02 billion people that already don't have enough to eat [29, 30, 88], many species are approaching their limits of extinction and the accelerated global warming effects are becoming more evident [95]. Somehow, we are

still getting it wrong; all the joint efforts of our governments and international agencies are failing in reversing our current destructive trends.

Angela Espinosa and Jon Walker [29] argue that the sustainability of a human society is based mainly on the way the society is organised rather than its relationship with the environment. They strongly believe that governments as they are, cannot manage a transition to a sustainable future. The hierarchical way with which governments operate is very ineffective in dealing with the high levels of complexity encountered at the lower levels of the society. They suggest that the way we govern ourselves needs to change to allow us to cope with the complexity of our society and that of the environment in which we live.

Stafford Beer, a teacher and colleague to both Espinosa and Walker, was a pioneer operational researcher and cybernetician who observed that the top-down approaches that governments use are not adept to handle the intricacy of societies' problems. Beer suggests to take a look at the natural world for successful examples of survival under complex conditions [9, 79]. He took inspiration from systems theory.

A system is a set of parts or elements that is coherently interconnected and organised in such a way that its structure leads to a characteristic set of behaviours. These are often the less obvious outcomes of the actions and are considered the function of the system; the system is more than the sum of its individual parts. Once the relationship between the structure and function of the system is understood, we can make inferences about how the system performs to tackle the tasks it undertakes and more importantly how it can improve this mechanism to produce better results. Systems, whether small or large, can behave in similar ways and in understanding these similarities or even differences we are taking the first step in making any lasting changes to the systems in which we are embedded [53]. The Earth

itself is a system made of many “living systems nested and embedded within smaller or larger systems” [29, 53], which are all expert in coping with the high level of complexity of their environment by self-regulating and adapting to any changes either externally or internally induced [89]. Human societies can learn a lot from the fundamental principles of governance in the systems of the natural world.

2.4 Seeking Sustainability in an age of complexity

Modelling communities as complex systems can help us understand how they evolved to the live structures we have today and thus help us manage their complexity. Stafford Beer was a pioneer operational research theorist and one of the first academics to apply complexity theory to the notion of sustainability. He explained that one needs to manage the complexity of a system in order for the system to become more sustainable and by using Ashby’s Law of requisite Variety[3] [1] he concludes that the right structures need to be in place to assist in managing the variety of the system. From this cybernetic[4] viewpoint the government has the role of the facilitator of change that emerges from actions at the local level [29]. Policy making in this respect is created with the view of enabling this change.

Beer developed the Viable Systems Model inspired by the brain and how it works perfectly as an autonomous system whose recursive organisational structure enables it to function in an ever changing environment. This model is in fact applicable to governments and institutions within the society, where they are viewed as recursive self-organising systems

[3] Ashby’s Law of Requisite Variety states that for a system to reach stability it must have a greater number of states in its control mechanism than the states that exist in the system that need to be controlled [1].

[4] Cybernetics stems from the Greek verb κυβερνάω(kybernáo) meaning to steer or govern; it was coined by Norbert Wiener in 1948 to describe the transdisciplinarry approach exploring the structure and dynamics of systems and "the scientific study of control and communication in the animal and the machine" [96].

that evolve in direct communication with each other and the environment in which they live in [9, 29].

The Viable Systems Model was applied successfully in at least two cases to map and manage the complexity of the countries of Columbia in 1998, in order to provide an intervention in the management of public performance, and Chile in 1972, to put in place a regulatory system for the social economy and mitigate the economic crisis that Chile was facing at the time. The latter example is of great importance as it enabled each nested system in the social economy to be self-regulated and autonomous to make decisions, whilst being updated in real time on information from different levels of the economy that it might affect or be affected by. This real time information sharing on all nested systems in the economy made Chile the most advanced government at the time and even makes current methods of governance envious. Sadly, the military coup on the 11th of September 1973 brought this to an end and the hi-tech operations room, where economic information was received and used for making quick decisions, was destroyed.

Perhaps the most powerful lesson learned from this cybernetic approach to governance is that nested systems should be allowed to be self-regulatory with information sharing at all levels and one must build the capacity to act proactively in decision making and respond to change effectively and in a timely manner. A myriad of examples of systems with change and adaptation at their core comes from complexity theory. In complex systems, the interactions and feedback between individuals, communities and the environment allow for greater flexibility and adaptation [37, 60]. At this stage it is vital to take a step back to see what we can learn from complex systems, which are either sustainable or unsustainable, and investigate how they organise themselves and how they operate to survive in their ever changing world.

2.5 Summary

The Earth is a unique planet that self-regulates and provides a nurturing environment for all its living organisms. Humans are now the dominant species on Earth and have evolved to be the main planetary engineers, whose actions can cause irreplaceable damages to the other organisms and the Earth itself.

Sustainability, the ability to meet the needs of the present without compromising the ability of future generations to meet their needs [11], goes beyond environmental protection and sits at the crossroads between concerns for the global environment and global social justice. A sustainable development path is needed to sustain human progress into the distant future; it is not a fixed state and thus not a straight forward process as the sustainability in the macroscale really depends on the decisions that individuals take in the microscale.

Governments and international agencies are struggling to find and implement a long-term solution to all the problems that are arising due to our unsustainable ways of living. This is because they are attacking each problem individually instead of viewing human sustainability as a problem concerning the nature of society and the way it is organised. The top-down approaches that governments and international agencies use are not adept at handling the intricacy of the problem and thus (complex) systems' theory is proposed as an alternative approach.

The natural world is made up of systems and the Earth itself is a system made of many smaller living systems. Therefore, human societies can learn a lot from the fundamental principles of governance in the systems of the natural world. By modelling communities as complex systems we can understand, and thus manage the complexity of the problems we

are facing.

Με το βουνό θα γίνω φίλος και με τα πεύκα σύντροφος.

Κι όταν θα κλαίω και πονώ θ΄ αναστενάζει το βουνό.

Ευάγγελος Πρέκας[5]

[5]Translation: I will become friends with the mountain, and a companion of the pine trees. So that when I cry and suffer, the mountain will sigh.

Chapter 3

Complexity and Networks

3.1 Reductionism Limitations

Reductionism is the philosophical belief that a system is nothing more than the sum of its individual parts. In the philosophical text *A Discourse on the Method*, René Descartes [23], a mathematician of the 17th century and also a prime practitioner of the reductionist approach laid out his scientific method in four steps:

1. "never accept anything for true" unless you prove it yourself
2. "divide each of the difficulties under examination into as many parts as possible, and as might be necessary for its adequate solution"
3. direct the "thoughts in such an order that, by commencing with objects the simplest and easiest to know, I might ascend by little and little, and, as it were, step by step, to

the knowledge of the more complex”

4. review the long chain of argument frequently to make sure nothing was omitted.

This four step process to the scientific method summarises the predominant approach to science until the beginning of the twentieth century. Scientists believed that they can draw firm conclusions about a system by simply understanding the mechanisms and purpose of its individual constituents, and have thus looked for the reductionist reasoning of all natural phenomena from the proven theories of fundamental physics. Sure enough, the application of the underlying principles of fundamental physics was very fruitful in explaining much of the phenomena scientists observed, with the only shortcomings appearing when scientists tried to apply these to the “complex phenomena closest to our human-scale concerns” [54].

Examples in which the reductionism approach has failed can be found all around us: from the way the actions of neurons give rise to the intricate behaviours in the brain, to the way colonies of millions of ants self-organise without the need of a central conductor to perform a particular task and the unpredictable behaviour of human societies in the political and economic domain. What is common in all of these examples is that we observe a complex behaviour that arises from the often simple interactions of a large number of components. In response to the shortcomings of reductionism theory the scientific community started leaning towards the idea that understanding the role of individual parts of a system does not necessarily help you predict the behaviour of a system. Scientists started coming together to look for interdisciplinary approaches to the problems they faced. As a result, new fields were created and old fields were looked at with fresh eyes which enabled science to go beyond the reductionist approach and start solving problems closer to our human scale concern in biology, economics and sociology [54]; a small list of these fields includes systems science and cybernetics which led the way to complex systems, or complexity science, and network

theory.

There are clear limitations to our knowledge of the underlying systems and all the myriad of feedback loops that cause the intrinsic behaviours observed, so a reductionist approach is impossible. If one wants to know more about the system and obtain quantitative information about it then a complexity approach is needed. To solve the most difficult problems of our generation such as sustainability, disease spreading and climate change one needs transdisciplinary methods to understand and explain the complexity.

3.2 Complexity Science

The word complexity takes its roots from the latin word *complexus* that means to embrace, or comprise of different intertwined elements [19]. A complex system is one consisting of many individual parts with often simple behaviour that are intricately interwoven in a non-linear manner that causes surprising emergent behaviours and patterns.

Complexity science is an interdisciplinary area of research with the aim of building a universal understanding of the characteristics that cause the emergent behaviours arising from the actions of large collections of simple entities, which self-organise into a collective whole that is more than the sum its parts [16]. The plethora of complex systems that exist in nature and the natural world, such as insect colonies, economies and the Earth, make this a fun yet non-trivial task.

3.2.1 Insect Colonies

Social insect colonies are nature's oldest and most successful complex systems. A single army ant has one of the simplest behaviours observed in nature, it will walk around looking for food, fight enemies and respond to chemical signals. Even in large numbers, say in the order of a hundred, ants exhibit behaviour that is aberrant and not worthy of special note; they will simply walk around aimlessly until they exhaust themselves to, literally, death [31]. Surprisingly, in extremely large numbers in the order of a hundred thousand the *Eciton* army ants can manage unimaginable things like transport large prey back in time for winter, traverse a tropical rainforest with perfect sense of direction and build long bridges using their bodies to allow other members of their colony to cross difficult terrain. They have biologically evolved to do this by utilising intelligence that has arisen as a property of collective cooperation and communication [31, 35] and only because it increases their probability of survivability as a species.

Ants are highly social, just like humans, and have evolved into "creatures with such an enormous contrast between their individual simplicity and their collective sophistication" [54]. They have been around for an estimated 140 million years [39] in comparison to homo sapiens 0.25 million years. In relative terms, if ants have been around for 1 day, humans have existed for a mere 2 minutes and 34 seconds. In addition, the biomass of ants is estimated to be roughly equal to the biomass of humans [18, 39]. Scientists have made substantial progress in understanding how social insects - be it ants, bees or even humans - work as a team [58], divide labour [76] and communicate [18, 75, 76], but cannot to this day fully explain exactly how their individual or collective behaviour came to be. Humans still have a lot to learn about complex systems and sustainability from taking a peek into insect colonies.

3.2.2 Economies

Economies are human made complex systems that have evolved over time to the structures we see today. They are made of simple economic entities - be it companies or individuals - who are producing or consuming goods. At the microscale, these entities are simply trying to increase their profits by gathering relevant information about the behaviour of other entities within the economy. At large numbers this behaviour becomes very complex and leads to the unpredictable behaviour of markets and fluctuations in prices and production of goods. Ideally, according to macroeconomic theory, the self-organising property of markets that emerges from the microscopic interactions of the companies and individuals should pull the economy into an equilibrium [54] and changes in production/consumption should be perfectly off-set by changes in the price of goods so that nobody is better off as a result of these fluctuations.

Real-world economies are seldom in equilibrium, and thus economists are always interested in what breaks this theory and makes economies inefficient. A complex systems approach to economics seems appropriate based on the description of complex systems observed elsewhere, namely that simple intricately connected components in the microscale lead to unexpected patterns in the macroscale, which in this case are global shocks to the economy, bubbles and subsequent crashes.

Another very relevant view is that the economy is in fact embedded in social networks [10, 36]. The personal links between the entities in the economy is of equal or at times higher importance than general economic transactions, mainly because these are not occurring solely between independent and impartial individuals but in fact between social entities that are connected over space and time. Analysing the structure and dynamics of the social

networks between individuals and companies in the economy can give an insight into the behaviour of their transactions.

3.2.3 The Earth

The Earth is a complicated complex system composed of many interacting components, many of them which are interconnected subsystems themselves. These include natural systems, like the atmosphere and biosphere, and also socio-economic systems like the ones discussed above. The Earth system is particularly difficult to predict for two key reasons. Firstly, it is dominated by the non-linear interactions that exist both within and between its components [95]. Secondly, the unpredictable human behaviour plays an integral part in how the system changes.

Humans play a powerful role within the Earth system; their large numbers and span of activities creates enormous complexity in the system as a whole making it difficult, or even impossible, to predict exactly the outcomes of the ever increasing pressure on the system. Their deep embeddedness and interconnectivity can have a great impact on the system and cause changes which unfortunately are not uniformly distributed, meaning that some parts of the Earth and some people are affected disproportionally too much.

Change in the Earth systems occurs in a non-linear manner, where feedback loops can either reinforce chance or completely dampen it [80]. To prevent negative change, be it social, economic or environmental, one must investigate and understand the Earth system as a whole, including the intricate interweaved connections between its components [95]. Therefore, the traditional top-down approaches to problem solving will fall short here as they are not flex-

ible enough to address these non-linear changes. After two decades of tackling sustainable development issues ineffectively, by targeting what we thought were isolated issues [29, 95], it is now time to integrate complex systems thinking into any sustainability conversations and decision-making processes.

3.3 Adaptability of Complex Systems

Simple systems can be broken down using a reductionist approach and their structure and dynamics can both be pinned down exactly. Their behaviour is predictable and can be calculated exactly by using simple cause and effect. Simple systems are mostly closed systems, which do not interact with their surroundings and thus do not need change in response to external factors.

Complex systems are made of many entities, some of which can be smaller nested systems. Above we saw how the Earth can be broadly broken down into natural systems, such as the atoms, oceans and ant colonies, or socio-economic systems like the economy, cities and political systems. These are all inter-connected meaning that they share information and influence the development of one another [95]. Adaptation is fundamental, as changing their behaviour increases their survivability [54].

In socio-economic systems a key component is humans, as their activities impose boundaries, structure, laws and other rules. The individuals embedded within the systems have the ability to think about their behaviours, reflect on their actions and change in response [37, 95] to what they think the best course of action is: a crisis can turn into a learning opportunity.

3.4 Emergence

Emergent behaviour has appeared a few times throughout this thesis already, in the examples of social insect colonies, economies and the Earth [2]. In all of these examples, simple rules on the individual components on the microscale level lead to complex, unexpected patterns seen in the system as a whole in the macroscale level [54]. The primary cause that gives rise to the emergent behaviour is the intricate underlying connections between the individual entities that cause long spacial and temporal correlations in the system. This means that the emergent properties are not predictable from even complete information of the microscopic entities [37], since the system cannot be broken down into non-interacting linear parts that are not sensitive to their environment.

The non-linear interactions and sensitivity to the environment are in fact the essential conditions for emergence [37, 95] and they exist both within and across all the complex systems of interest with respect to sustainability, such as the environment, the economy, society and even government and other institutions. A more formal method of analysing and understanding these interactions is key to understanding the emergent behaviour of the system as a whole.

3.5 Network Science

Most things in the world can be represented as pair-wise interactions between elements in the system. Mathematically the interactions are represented by links (also known as edges), the elements are represented by nodes (also known as vertices) and the collection of these

is called a network [59]. It should be of no surprise that examples of real world networks are found all around us, including neural networks in the brain, airline flight routes, social media friendships or even all the routers that together make up the backbone of the Internet [92]. Social communities are networks whose nodes are people or sometimes groups of people and can have many different types of relationships between them that are of interest to our sustainability or even survival, such as identifying and analysing terrorist networks as a matter of national security [73, 74, 97].

The structure of networks has been studied in isolation by many fields for hundreds of years, in the context that was appropriate in their respective discipline. For example, in mathematics networks takes the form of graph theory [84], in epidemiology it is disease spreading due to direct person-person interactions [15] and in economics it is the spread of technological advancement and expertise across businesses [12, 54]. Over the last two decades, researchers have been coming together to investigate networks of all forms, to find a set on unifying principles that apply to them and develop methods by which to analyse them. This is what now has developed into the science of networks [59].

Common language was created to consolidate the existing work on networks stemming from different fields and allow for better communication between researchers. Some of the most important network terms, that will appear elsewhere in this thesis, will be introduced here; to assist in this task I created the social network of the people (nodes) mentioned in my acknowledgements, numbered in order of appearance in the text, see Fig. 3.1.

Clustering refers to the tendency nodes have to create separate communities within a network. In my acknowledgement social network (Fig. 3.1) there is a clear divide between my academic (grey) friends and all others.

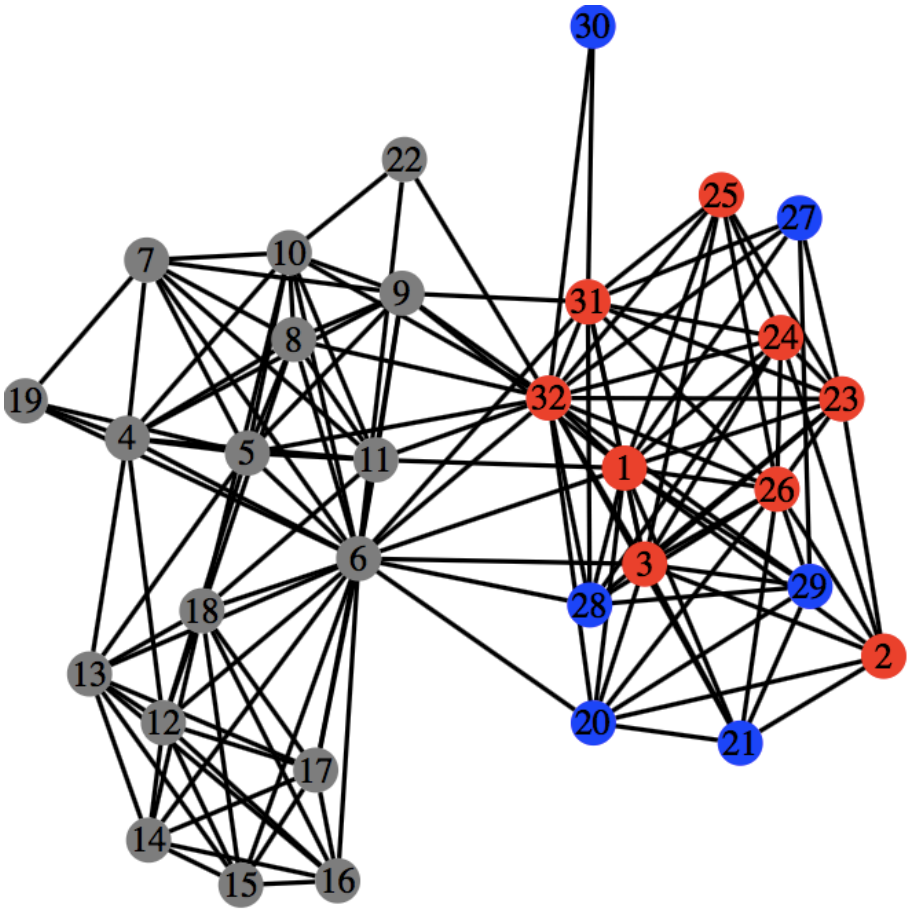


Figure 3.1 **Network of acknowledgements.** The social network of the individuals in the acknowledgements section, where nodes are numbered in order of appearance in the text and coloured according to whether they are family (red), academics (grey) and close friends (blue). The average path length is 1.86 and the average degree is 9.3. Node 6 is a hub node, as it is connected to 70% of the other nodes in the network and its degree (22), greatly exceeds the average. It also has the highest betweenness centrality (166), which means that it acts as the predominant bridge along the shortest path between most pairs of nodes.

The *degree* of a node is the number of links the node is attached to. Accumulating all of these together allows for a degree distribution to be defined. *Hubs* are high-degree nodes that have an important role in propagating information across the entire network. For example, in Fig. 3.1 node 6 is connected to 70% of the nodes and its degree (22) greatly exceeds the average degree (9.3) of the network.

The *path length* is the shortest distance between two nodes, which is calculated by the number of links that you need to traverse to get from one to the other. And thus, the *average path length* is simply the average over all pairs of nodes. In the network shown in Fig. 3.1, the average path length is 1.86 implying that on average you can get from one node to another using less than two edges. The *betweenness centrality* of a given node is the times a node acts as a bridge along the shortest path between two other nodes and is normalised over the total number of shortest paths between all pairs of nodes. Effectively, nodes with high betweenness centrality typically act as bridges between clusters. Unsurprisingly, given its degree, node 6 in the acknowledgement network is the most central with a betweenness centrality of 166 and is the main link between the clusters. Centrality measures, like degree and betweenness, aim to identify key nodes based on their relationship with other nodes in the network.

Most real world networks studied thus far, whether they are social, natural or technological, seem to have similar characteristics: high-clustering, scale-free degree distributions and hubs [54]. *Scale-free* networks have power-law degree distributions, *i.e.* they can be expressed according to

$$P(k) \sim k^{-\gamma}, \tag{3.1}$$

where γ is the scale-free exponent. The distribution is self-similar, meaning that it has the same shape whether you have a thousand nodes or a million nodes, and hence they do not have a characteristic scale.

Popular scale-free networks are the World Wide Web, social networks and networks of businesses. It is thought that they have developed into this interesting structure because they grew into this shape with preferential attachment, meaning that new nodes entering the network prefer to attach themselves to higher-degree nodes already in the network. This

increases the survivability of the node in a new environment. Some of these concepts will be re-iterated in Chapter 6, where the real-world network between firms of an economy will be introduced.

3.6 Summary

Reductionism was the main approach to all scientific problems and proved very successful until it was applied to human-scale phenomena. Scientists believed that nothing was more than the sum of its parts, and thus it could be broken down to its individual components, studied separately and then put back together to draw conclusions about the whole. The common denominator in all the cases where reductionism has failed is that a complex behaviour arises as a result of the often simple interactions of a large number of components, such as the unpredictable behaviour of human societies in the political and economic domain.

Such systems are called complex systems and complexity science is the transdisciplinary discipline that has been given as an appropriate method for their scientific investigation. Its sole purpose is to build a universal understanding of how large collections of simple entities self-organise into a collective whole that is more than the sum its parts [16]. Many examples of complex systems exist in nature, such as ant colonies that self-organise to take care of their brood, economies that have unpredictable market behaviours and the Earth that is affected disproportionately by the actions of man.

The entities in complex systems are all inter-connected and therefore, they can use information, and, in some cases, evolve and learn. In socio-economic systems, for example, the

individuals embedded within the system are able to think about their behaviour and adapt in order to increase their survivability [37, 95]. The pair-wise connections between the entities can be represented using networks, where the entities themselves are the nodes and their interactions are the links joining them. Network descriptions of systems exist everywhere [59, 92], including for socio-economic communities whose nodes are people or businesses and can have many different types of relationships between them, such as the exchange of money and goods in the economy and even criminal or terrorist affiliations in a social network.

Network science is an area of research that investigates networks of all forms and aims to find a set of unifying principles that connects them and scientific methods to analyse them. Most real world networks have a common set of characteristics: high-clustering, scale-free degree distributions and hubs. It is thought that scale-free networks developed into this structure because they grow with preferential attachment, *i.e.*, because the grew into this shape with preferential attachment, meaning that new nodes entering the network prefer to attach themselves to higher-degree nodes already in the network. One such scale-free network is the trade network of the economy.

Chapter 4

The generalised sandpile model as a paradigm for economic activity

Part of the material presented in this chapter was published in a peer-reviewed journal, where all contributing parties have been properly acknowledged [98]:
Zachariou, N., Expert, P., Takayasu, M., and Christensen, K. (2015). Generalised Sandpile Dynamics on Artificial and Real-World Directed Networks. PLoS ONE, 10(11):e0142685.

4.1 Introduction

The observed large fluctuations in aggregate economic activity proves to be one of the oldest problems of macroeconomic theory, especially since these can arise as a result from many small, predictable and independent shocks to individual sectors [77]. The instability in the

economic aggregate is not the result of drastic change in behaviour, but is instead induced from a fairly constant demand of goods. For this reason, understanding it is of great interest to economists, as the shocks cannot be predicted and planned against and this leads to a very expensive inventory management and non-ideal ad-hoc scheduling at the production level [14, 77].

Uncovering the mechanisms that lead to these large scale fluctuations is by no means an easy task since these are deeply hidden in the behaviour of the whole economy. It is reasonable for one to expect that different parts of the economy must be independent and thus any independent shocks in different sectors will just die out in the noise leading to Gaussian distributed fluctuations in the aggregate. Interestingly, this is not true, which leads to the hypothesis that the seemingly independent parts of the economy may not be so independent after-all and that non-linear and localised interactions may exist between them. Self-organised criticality (SOC) has been proposed by Scheinkman and Woodford [77] and Bak *et al.* [7] as a paradigm to explain the large fluctuations observed on all scales that were caused by small independent shocks to individual sectors.

What does self-organised criticality actually mean? Self-organised criticality, a term coined by Bak, Tang, and Wiesenfeld (BTW) refers to systems with many degrees of freedom that spontaneously reach a dynamically critical state when slowly driven [5]. The system has two characteristic timescales, the slow one where the system is driven from and the fast one where the activity in response to the driving takes place.

To understand this metaphorically, let's consider a pile of sand. If one grain of sand at a time is dropped consecutively at the top of a table, eventually, a sandpile will emerge that organises itself to reach a critical point where one sand grain can cause an avalanche of

any size to topple down the slope. The avalanche size is simply the number of grains that were involved in the toppling. That is, after the system goes through a transient period, the system reaches stationarity. Once in the steady state, the frequency of avalanches yield a scale invariant avalanche size probability density function (pdf) [5]. This behaviour is not only observed in sandpiles, but also in aggregate economic activity [77] and is abundant in nature [2, 41], ranging from the coevolution of species [3], to earthquakes [4, 8], to lung inflation [82] and even rainfall [68].

An entertaining sandpile style scenario emerges when thinking about a large office of bureaucrats. Imagine that the desks of the bureaucrats are arranged in perfect rows, see Fig.4.1, where all bureaucrats apart from the ones sitting at the edges have four nearest neighbours. When a piece of paper enters through the door it will land at the desk of random bureaucrat and will require some action. The bureaucrat will not deal with it until at least four pieces of paper have piled on his desk, at which point she will pass one piece to each of his nearest neighbours. All bureaucrats behave according to this rule, with the exception of the ones sitting near the windows, who simply throw the piece of paper out of the window and onto the street. Once there are enough papers in the system, it will reach a point where one additional piece of paper coming through the door will lead into a chaotic process of paper transfer sequences. In the modern working environment, emails have replaced pieces of paper and bureaucrats do not have just four nearest neighbours but instead are frequently carbon copied into the scale-free (see Sec. 3.5) email networks of their colleagues; this must surely create avalanches of extreme measures[1].

A self-organised critical system that has reached the critical state, like the ones described above, can only relax by a burst of activity. In the (original) sandpile example this is when

[1] After working for Her Majesty's Government for nearly two years, I can neither confirm nor deny this conjecture. If true, however, it would explain most of the problems that I have experienced with human resources thus far.

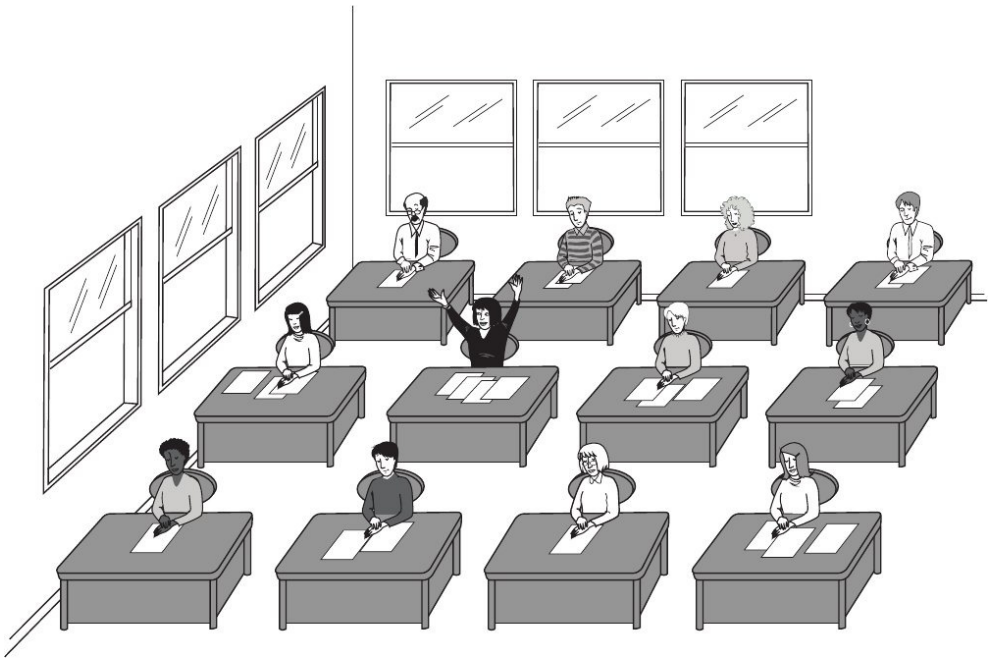


Figure 4.1 **Illustration of a sandpile in bureaucracy.** Bureaucrats remain inactive until four or more pieces of paper requiring action are found on their desk, at which point they will send one piece of paper to each of their nearest neighbours. After some time, the system will reach a point where a single piece of paper entering the office will cause an avalanche of papers being shuffled around. This light-hearted application of the sandpile to a bureaucratic setting is courtesy of the physicist Peter Grassberger who, ironically, is famous for his research in chaos theory.

an avalanche of sand grains topple down the slope. At the critical state, there are long-range temporal and spatial correlations even though only direct short-range interactions among the constituents are permitted. The system is scale invariant, which means that all scales are of equal importance and that the landscape of the sandpile in its current form depends on all of its history, but also constraints the whole future evolution. Mathematically, the avalanche sizes y display finite-size scaling (FSS), meaning that a power-law can be fitted, where the pdf follows the expression

$$P(y;L) = y^{-\tau}\mathscr{G}(y/L^{D}), \tag{4.1}$$

for $y \gg 1$ and $L \gg 1$, $\mathscr{G}$ is a universal scaling function and the critical exponents D and

τ are the avalanche dimension and the avalanche-size exponent, respectively [5, 72]. The conditions $y \gg 1$ and $L \gg 1$ effectively mean that the system is in the thermodynamic limit, where corrections to scaling (for finite system sizes) can be ignored.

A special case of the BTW model is the directed sandpile model, where the flow of motion has a strict directional rule and can not be reversed [72]. The dynamics exhibit the same characteristics: criticality, scale invariance and finite-size scaling. It was proven analytically by Dhar and Ramaswamy that the avalanche-size pdfs of a directed sandpile model on a two-dimensional lattice fit the FSS Eq. (4.1) with scaling exponents $\tau = 4/3$ and $D = 3/2$ [26].

It bears similarities to other models of non-equilibrium statistical physics like the Takayasu's model of aggregating and diffusing particles with injection, the Scheideggar river network model, the voter model [25] and the growth of falling rain droplets [68, 69].

Bak, Chen, Scheinkman and Woodford [7] redefined the dynamics of the classical two-dimensional directed sandpile to model intersectoral trade. They recovered $\tau = 4/3$ and $D = 3/2$ whilst investigating the fluctuations in the production. Whilst this work was pioneering for its time, it nevertheless only considers a very rigid topology and homogeneous producers each joined to only two consumers and hence, essentially, is simply putting the directed sandpile model into another (very relevant) context. However, allowing for a more realistic setting where a more general pattern of connectivity among producers and consumers is possible, and then increasing the number of producers that each consumer is connected to, should cause longer chain reactions [77].

In the current chapter, the dynamics of the directed sandpile model [7, 26] is adapted to

cover for different number of producers and consumers, with the potential of running the dynamics on any directed topology [98]. Then, the generalised dynamics is investigated numerically and theoretically on regular, strictly layered lattices (Chapter 4 and Chapter 5). However, the most realistic topology one can use for studying intersectoral trade is in fact the production-consumption network between firms in a real economy, which is done in Chapter 6.

4.2 Model definition of the generalised sandpile

Bak *et al.* [7] showed that the classical two-dimensional directed sandpile model is applicable to the study of the fluctuations in the production of intersectoral trade. In their adaptation, the economy takes the form of a cylindrical lattice with L layers and each productive unit has only two suppliers directly connected in the layer below and two consumers directly connected in the layer above, see Fig. 4.2. If a productive unit is activated and needs to produce, it will create and transfer two units of output, one to each of its two customers by utilising two units of input, taking one from each of its two supplier units. The productive unit is also allowed to keep units in its inventory, although to optimise the costs of keeping the inventory it can hold a maximum of one unit of product. Production starts only when an order from a customer node in the layer above cannot be fulfilled exclusively from the products stored in the inventory.

Just like dropping a grain of sand at the top of the pile, this system is driven by independently shocking a node in the first layer of the cylindrical economy, see Fig. 4.2. The distribution of aggregate production behaves exactly like the avalanches in the directed sandpile as discussed above, and moreover the critical exponents $\tau = 4/3$ and $D = 3/2$ are recovered

[7, 77]. Thus, this simple model is useful in reproducing certain traits and behaviours of the macroeconomy, but the issue still remains that the underlying network is very unrealistic and rigid.

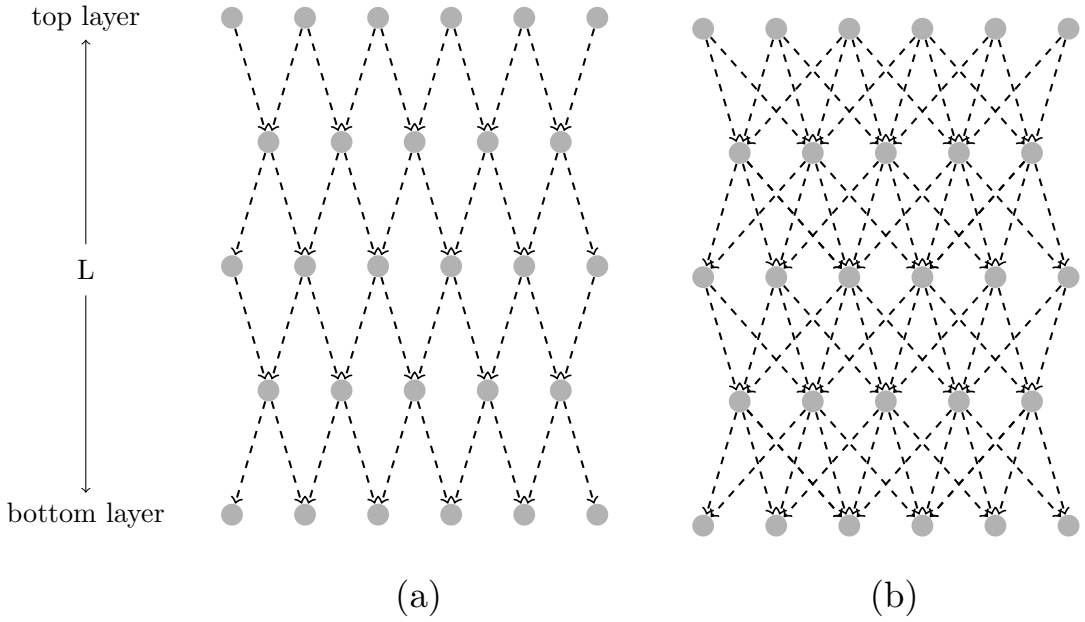


Figure 4.2 **Illustration of regular lattice topologies.** Networks shown are subsets of: (a) a two-dimensional directed lattice with coordination number $K = 2$; (b) a two-dimensional directed lattice with coordination number $K = 4$. Periodic boundary conditions are applied to the left- and right-most nodes to form a cylindrical structure. The nodes in the top layer are the final goods producers, the nodes in the bottom layer are providers of raw materials and all other nodes between are the producers of intermediate goods. It is left to the readers imagination to extend this setup to higher co-ordination numbers $K > 4$.

The first improvement that one may want to do is allow for an increased number of suppliers and customers that a productive unit may be directly related to. To allow for this, the dynamics that were introduced by Bak, Chen, Scheinkman and Woodford [7] for a directed two dimensional lattice with co-ordination number $K = 2$ will need to be adapted to allow for a more general lattice structures and higher coordination numbers.

Let us define an economy consisting of N productive units that are arranged in L number of layers on a lattice, with periodic boundary conditions connecting the two vertical edges and tracing the shape of a cylinder, see Fig. 4.2. By definition, the circumference M of the lattice, where $M = N/L$, is also the width of the economy.

Each productive unit is identified by its coordinates in the lattice, denoted by (i, j), and has a set of suppliers in the layer below to buy supplies from and a set of customers in the layer above to sell products to. Viewing these relationships as a network, then at (i, j) there exists a node with unweighted directed links (n, n') connecting each supplier node $n(i, j)$ to each of its customer nodes $n'(i', j')$. Therefore, the set of customers of node $n(i, j)$ is simply

$$N_{i,j} = \{n'(i', j') \mid n'(i', j') \text{ is a customer of } n(i, j)\}. \tag{4.2}$$

The out- and in-degrees of each node $n(i, j)$ are $k^{out}_{i,j}$ and $k^{in}_{i,j}$, respectively, and are simply the number of suppliers and customers of each productive unit. In the special cases shown in Fig. 4.2, we have $k^{out}_{i,j} = k^{in}_{i,j} = 2$ and $k^{out}_{i,j} = k^{in}_{i,j} = 4$, respectively. The network of the entire economy can be traced by accumulating together all the nodes with their respective links. In this layered network economy, the nodes in the top layer are the final goods producers, the nodes in the bottom layer are providers of primary raw materials and all other nodes between these two layers are the producers of intermediate goods. Fig. 4.2 shows a snippet of such a network.

The system is driven from the top layer and at each time step a node in the network may be activated if the avalanche reaches it and also may be required to sell product to its customers. Production is required when a customer's order cannot be met solely using products from the inventory of its supplier. For $n(i, j)$, define $x_{i,j}(t)$ to be the state of the inventory at time

t, $y_{i,j}(t)$ to be the quantity of goods produced at time t and finally, $s_{i,j}(t)$ to be the number of goods sold at time t. When node $n(i,j)$ receives an order from a customer in the layer above, it will check its inventory to see whether it can fulfil the order from the product in its inventory, without having to produce. If it does, then it just sells a unit of product to its customer and does not produce anything, *i.e.* $y_{i,j}(t) = 0$, see Fig. (4.3)(a). If it does not, then it must start production to cover for potential orders from all its customers and $y_{i,j}(t) = k^{in}_{i,j}$, see Fig. (4.3)(b). Note that regardless of the amount of units a node produces, it will only give its customer one unit and conversely, regardless of how many units of material a customer requires, it can only ask for one unit from each supplier.

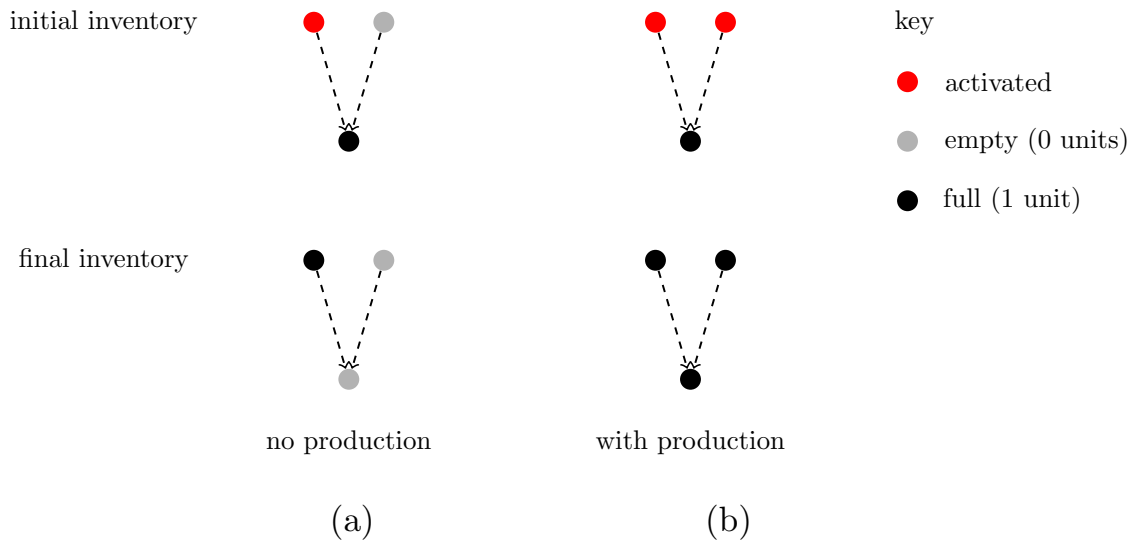


Figure 4.3 **Illustration of a local process with and without production.** Networks shown are subsets of a two-dimensional directed lattice with coordination number $K = 2$ with different initial inventory configurations: (a) the producer node (black) receives an order from its customer, the activated (red) node in the layer above, and since it can fulfil the order from the product in its inventory it will simply hand it over and not go into production, $y_{i,j}(t) = 0$, resulting in an empty inventory in the final configuration; (b) the producer node (black) receives two orders from both its customer, the activated (red) nodes in the layer above, and since this time it cannot fulfil both orders from the product in its inventory it must produce to its full capacity, $y_{i,j}(t) = k^{in}_{i,j}$ which is 2 units in this case, and give the product to its customers leaving all inventories full in the final configuration.

The variables of interest are no longer homogeneous and in fact their values are dependent on the in- and out-degrees of each individual node: the inventory is $x_{i,j}(t) \in \{0,\ldots,k^{in}_{i,j}-1\}$, the production is $y_{i,j}(t) \in \{0,k^{in}_{i,j}\}$ and the sales are $s_{i,j}(t) \in \{0,\ldots,k^{in}_{i,j}\}$. To avoid dissipation each node must have at least two customers and two suppliers, *i.e.* $k^{in}_{i,j}, k^{out}_{i,j} \geq 2$.

The inventory $x_{i,j}(t)$ is updated at each time step by adding the number of units it produced and subtracting the number of units it sold, *i.e.*

$$x_{i,j}(t+1) = x_{i,j}(t) + y_{i,j}(t) - s_{i,j}(t), \tag{4.3}$$

where $s_{i,j}(t)$ are driven by the accumulated orders coming from all active customer nodes $n'(i',j')$ of each node $n(i,j)$ at that time-step, *i.e.*

$$s_{i,j}(t) = \sum_{n'(i',j')\in N_{ij}} \frac{y_{i',j'}(t)}{k^{in}_{i',j'}}. \tag{4.4}$$

An avalanche is the total size of production $y(t)$ and is calculated by summing together all the individual productions of all the nodes $n = 1,..,N$ in the economy:

$$y(t) = \sum_{n=1}^{N} y_{i,j}(t). \tag{4.5}$$

Note, that not all nodes contribute to this sum at every time step as they may not have needed to produce.

4.3 Theoretical framework

The size of an avalanche can only be predicted if one has complete knowledge of the structure of the network and the entire inventory of all nodes in the system. However, this is a cumbersome task and not necessary as the statistics of avalanche-size pdfs behave according to well-defined laws [72].

Assume that the avalanche-size pdfs obey FSS, meaning that a power-law can be fitted, that is, it can be expressed in the form

$$P(y;L) = ay^{-\tau}\mathscr{G}\left(y/L^{D}\right) \quad \text{for } y \gg 1, L \gg 1, \tag{4.6}$$

where τ and D are universal scaling exponents, $\mathscr{G}$ a universal scaling function and a a non-universal dimensionful parameter that is independent of the lattice size L.

Simple manipulation of Eq. (4.6) yields

$$y^{\tau}P(y;L) = a\mathscr{G}\left(y/L^{D}\right). \tag{4.7}$$

Plotting the transformed pdf $y^{\tau}P(y;L)$ against the rescaled observable y/L^{D}, would mean that all the data collapses onto the curve of the scaling function $\mathscr{G}$. This of course is only possible if the data for the different system sizes L are consistent with the FSS ansatz.

The avalanche-size scaling exponents τ and D can be estimated using moment analysis. Assuming that the FSS ansatz holds for pdfs y, then the kth moment can be estimated using Eq. (4.7) as follows:

$$\begin{aligned}
\langle y^k \rangle &= \sum_{y=1}^{\infty} y^k P(y;L) \\
&= \sum_{y=1}^{\infty} a y^{k-\tau} \mathscr{G}\left(y/L^D\right) \\
&\propto \int_1^{\infty} y^{k-\tau} \mathscr{G}\left(y/L^D\right) dy \\
&\propto \int_{1/L^D}^{\infty} \left(uL^D\right)^{k-\tau} \mathscr{G}(u) L^D du \\
&\propto L^{(k-\tau+1)D} \int_{1/L^D}^{\infty} u^{k-\tau} \mathscr{G}(u)\, du
\end{aligned} \tag{4.8}$$

where the sum was approximated using an integral and the substitution $u = y/L^D$ was used.

As L tends to infinity, the integral in Eq. (4.8) will converge to a finite number; the integral is finite at the lower limit which is now 0, where the scaling function $\mathscr{G}$ converges to a constant, as long as the avalanche-size exponent satisfies $1 + k > \tau$; the integral is finite at the upper limit infinity because the scaling function $\mathscr{G}$ decays fast to ensure convergence [16]. Thus, the kth moments of the avalanche-size probability scale with the system size L according to the following relation

$$\langle y^k \rangle \propto L^{D(1+k-\tau)}, \tag{4.9}$$

for $L \gg 1$ and $k \geq \tau - 1$.

Plotting the measured moments $\langle y^k \rangle$ against system size L in a double logarithmic plot gives a straight line, where the slope is $D(1+k-\tau)$ for $L \gg 1$.

Then, plotting the estimated slopes $D(1+k-\tau)$ against k gives a straight line where the gradient is D, and the line intersects the k-axis at $k^\star = \tau - 1$, *i.e.* $\tau = 1 + k^\star$.

Moment analysis is used to estimate D and τ; these values are then validated by producing a data collapse according to Eq. (4.7). Also, due to conservation of the grains of sand and Eq. (4.9), the first moment (where $k = 1$) is expected to follow

$$\langle y \rangle \propto L^{D(2-\tau)} \propto L, \tag{4.10}$$

which means that the following scaling relation must hold true

$$D(2-\tau) = 1. \tag{4.11}$$

4.4 Results on a regular lattice with K ≥ 2

Numerical simulations were used to confirm that the generalised sandpile dynamics give the known results [7, 26] for $K = 2$, and then this setup was extend for higher coordination numbers $K > 2$.

The directed sandpile is relatively easy to implement numerically due to the fixed direction of avalanches, as by construction, there is no backward flow [42] or multiple topplings [63]. In the simulations that follow, three system sizes were tested $L = 200, 400, 600$ with constant

width $M = 2000$, unless otherwise stated. To bring the system into a steady state, a transient period of 5×10^5 avalanches was used, where simulations were allowed to run in order to eliminate initialisation bias from random initial configurations. Nodes in the first layer kept an empty inventory to ensure that each particle addition at the top resulted in a non-zero avalanche.

Moment analysis was conducted directly on the results of the simulations as described above. Logarithmic data binning was used to visualise the avalanche size pdfs by dividing the horizontal axis into bins labelled $j = 0, 1, \ldots$, where the jth bin holds all avalanches in the interval $[a^j, a^{j+1}[= \{r \in \mathbb{R} \mid a^j \leq r < a^{j+1}\}$. The bins are increasing exponentially in length for $a > 1$; here $a = 1.1$ was used. For bin j, let y^j_{min} and y^j_{max} denote the minimum and maximum integer avalanche sizes that it can hold and then calculate the number of avalanches that fall in within this interval $[y^j_{min}, y^j_{max}]$. Then, instead of plotting the avalanche size pdfs directly, $P(y^j; L)$ as defined below

$$P(y^j; L) = \frac{No.\ of\ avalanches\ in\ bin\ j}{N \Delta y^j} \tag{4.12}$$

is plotted against the geometric mean, $y^j = \sqrt{y^j_{max} y^j_{min}}$ of the avalanche sizes in bin j, where N the number of avalanches in the interval $[y^j_{min}, y^j_{max}]$ and $\Delta y^j = y^j_{max} - y^j_{min} + 1$ is the corresponding number of integers. Without the logarithmic binning, it would be impossible to extract any information from the extremely noisy tail of the pdfs [16].

In this generalised version of the sandpile model on a *regular lattice* with higher coordination numbers, we have that $k^{in}_{i,j} = k^{out}_{i,j} = K$, where $K \in \mathbb{N}^+$ and $K \geq 2$. The dynamical rules are as defined as in Section 4.2 but the constraints on the range of variables of interest are simplified as all nodes in the system have the same coordination number. The constraints are: $x_{i,j}(t) \in \{0, \ldots, K-1\}$ for the inventory, $y_{i,j}(t) \in \{0, K\}$ for the production

and $s_{i,j}(t) \in \{0,\ldots,K\}$ for the sales. The case where $K = 2$ reduces to the original model as defined in Bak *et al.* [7].

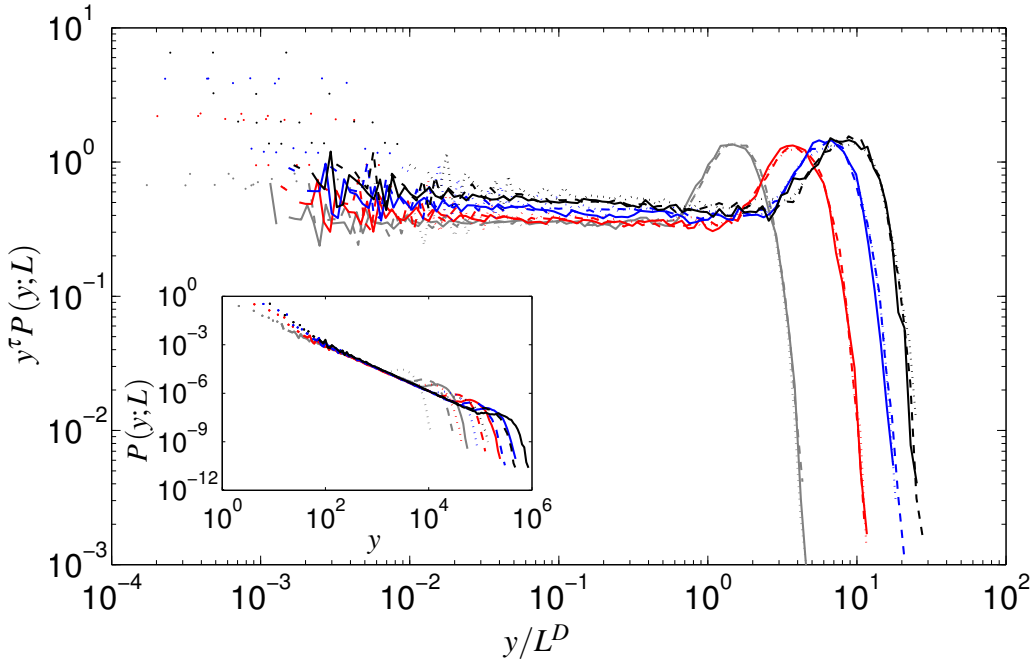


Figure 4.4 **Results on regular lattice with higher coordination number.** The main figure shows the data collapse for different coordination numbers K of the avalanche-size pdfs $P(y;L)$ obtained by plotting the transformed avalanche-size pdf $y^{\tau}P(y;L)$ against the rescaled avalanche size y/L^{D} using the estimates of the avalanche-size scaling exponents τ and D obtained from moment scaling analysis, see Table 4.1. The line style indicates the system size, dotted line: $L = 200$; dashed line: $L = 400$; solid line: $L = 600$. The width of the system is kept constant at $M = 2000$ nodes. The colours show the coordination number for the regular lattice underlying networks; $K = 2$ (grey), $K = 4$ (red), $K = 6$ (blue), $K = 8$ (black). The inset displays the avalanche-size pdf $P(y;L)$ plotted against the avalanche size y after logarithmic binning was used.

The numerical results show that avalanche-size exponents are consistent with the two-dimensional directed sandpile model universality class, $\tau = 4/3$ and $D = 3/2$ for all K. The avalanche size pdfs are displayed in Fig. 4.4 and in both figures it is evident that there

is a characteristic "bump" in their fat tails. This is to be expected, as it is due to finite-size effects that arise, because the bins that contribute to the bump have: (a) the avalanches of the appropriate size that have finished propagating and (b) in addition avalanches that would have carried on had the avalanche not hit the bottom (boundary) layer and would have been in another bin had the system not been finite.

K	M	τ	D	$D(2-\tau)$
2	2000	1.33(5)	1.47(10)	0.98
4	2000	1.35(5)	1.55(10)	1.00
6	2000	1.37(5)	1.60(10)	1.00
8	2000	1.39(5)	1.63(10)	1.00
8	4000	1.37(5)	1.61(10)	1.00

Table 4.1 **Scaling exponents on regular lattices.** The avalanche-size exponent, τ, and the avalanche-dimension, D, for regular lattice structures with coordination numbers, $K = 2,4,6,8$ and circumference M, see Fig. 4.4 for the data collapse. The numbers in the brackets indicate the estimated errors of the exponents. The scaling relation $D(2-\tau) = 1$, see Eq. (4.11), is fulfilled (see last column) and, within error bars, both scaling exponents (apart from $K = 8$ and $M = 2000$) are consistent with the universality class of the two-dimensional directed sandpile model $\tau = 4/3$ and $D = 3/2$. The numerical result for $K = 8$, $M = 2000$ and 4000 suggests that the apparent drift is due to finite size effects.

The associated scaling exponents, which were estimated using moment analysis, are listed in Table 4.1. Both τ and D are within error bars of the expected values of the two-dimensional universality class for all coordination numbers tested.

The avalanche-size scaling exponents τ and D seem to drift slightly as the coordination number K increases (see Table 4.1). Doubling the width of the lattice from $M = 2000$ to $M = 4000$ for $K = 8$ and brings the exponents closer to the ones with smaller coordination numbers. This suggests that the apparent drift is probably due to finite-size effects and thus one can deduce that the generalised sandpile model on a regular lattice falls within the classical universality class of $\tau = 4/3$ and $D = 3/2$ for all K. However, this argument

is hypothetical but can be made firm with a theoretical calculation, as will be shown in Chapter 5.

4.5 Summary

Understanding the observed large fluctuations in aggregate economic activity is an important issue in economics, as the shocks are very destructive and cannot be predicted or planned against [77]. Instead, they emerge as a result of many small, predictable and independent shocks to the individual sectors [14].

The mechanisms behind the large scale fluctuations are deeply hidden in the actions of the economic entities. The sandpile model, a self-organised critical [5] system with many degrees of freedom that spontaneously reach a dynamically critical state when slowly driven, has been proposed as a paradigm [7, 77] to model intersectoral trade. The avalanches of sand are analogous to the large fluctuations in production and just like dropping a grain on the top of a sandpile, this system is driven by small, predictable, independent shocks.

At the critical state the system is scale invariant, which means that all scales are of equal importance. The avalanche sizes y display finite-size scaling (FSS), that is, they follow a scaling form (see Eq. (4.1)) that has been analytically proven to have scaling exponents $\tau = 4/3$ and $D = 3/2$ [7, 26]. This model is useful in reproducing certain traits and behaviours of the macroeconomy, with the one draw back being its rigid underlying network.

Generalising the deterministic directed sandpile model and considering its dynamics on strictly layered lattices, where the out- and in-degrees of each node is increased to the co-

ordination numbers $K \geq 2$ (see Fig. 4.2), the classical two-dimensional directed sandpile model universality class, with $\tau = 4/3$ and $D = 3/2$ [7, 26] is recovered again. However, there seems to be an apparent drift in the avalanche-size exponents τ and D, which seem to increase slightly as the coordination number K increases (see Table 4.1). The apparent drift is probably due to finite-size effects, but a theoretical investigation is needed to confirm this (see Chapter 5).

Chapter 5

Analytical solution of the directed sandpile model for $K \geq 2$

Part of the material presented in this chapter was published in a peer-reviewed journal, where all contributing parties have been properly acknowledged [27]:
Dhar, D., Pruessner, G., Expert, P., Christensen, K., and Zachariou, N. (2016). Directed Abelian sandpile with multiple downward neighbors. Phys. Rev. E, ***93****:042107.*

5.1 Introduction

The sandpile model was introduced by Bak, Tang and Wiesenfeld [5, 6] and was the first model to display self-organised criticality. The directed sandpile model is a variation of the original model, where a preferred direction of toppling was imposed and it was solved ana-

lytically by Dhar and Ramaswamy [26] for the special case of $K = 2$. The critical exponents and the two-point correlation function were determined in all dimensions, d. For $d = 2$, $\tau = 4/3$ and $D = 3/2$ while for $d \geq 3$, the exponents take the mean-field values $\tau = 3/2$ and $D = 2$ [50].

Dhar and Ramaswamy's analytical solution [26] of the directed sandpile model on a regular lattice with coordination number $K = 2$ in dimension $d = 2$ is just a two particle annihilating random walk because the avalanches are compact and have no side branches and no holes.

It was observed in Chapter 4 that increasing the coordination number in Monte Carlo simulations led to a slight drift [98] from classical exponents of the known two-dimensional directed sandpile universality class, see Table 4.1 on page 76. The structural changes in avalanches for $K > 2$ mean that the argument for compact avalanches and two annihilating random walkers may no longer be valid as the obvious side branches create holes in the developing avalanches (Fig. 5.1). The typical avalanche clusters shown in the visualisations are qualitatively different in the cases where $K = 3$.

The question posed here is whether the observed drift from the classical exponents is attributed to structural differences between the avalanches from the $K = 2$ to the $K > 2$ setup that cause strong finite size effects, and if so, whether significant corrections to scaling are enough to prove that the system is in the same universality class for all $K \geq 2$.

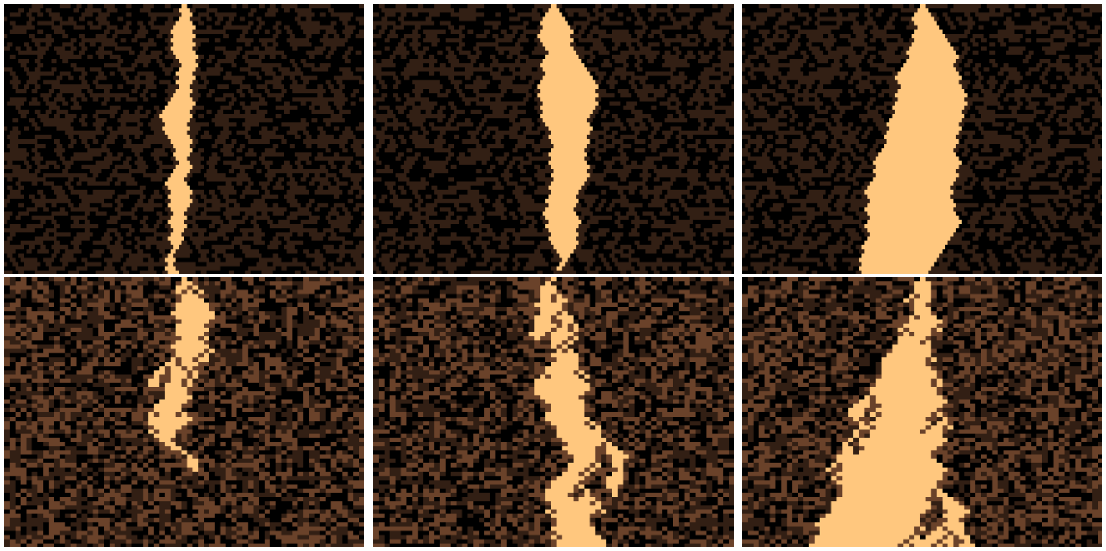


Figure 5.1 **Illustrations of avalanches.** Three randomly selected examples of avalanches for systems with co-ordination numbers $K = 2$ (top row) and $K = 3$ (bottom row), with avalanche sizes $s = 201; 406; 802$ and $s = 201; 404; 805$ respectively. The avalanches start at the top row ($t = 0$) and for display purposes have been centred around their seed node. The lattices used to generate these results have height $L = 64$ and width $M = 160$; only the middle 64 columns are displayed here as these are enough to show the trajectory of the avalanche. The toppled sites have an off-white colour and the remaining sites have different shades of brown based on their height at the end, when the avalanche has stopped. For $K = 2$ the allowed heights are $h(x,t) = 0, 1$ and for $K = 3$ a site does not topple for $h(x,t) = 0, 1, 2$. The avalanches for $K = 2$ are compact as opposed to the avalanches for $K = 3$. Also, notice the $K = 3$ avalanches can have side branches.

5.2 Model definition

As in Chapter 4, a directed sandpile model on a cylindrical lattice of length L layers and width (circumference) M is considered. Each site is given a label $\vec{X} \equiv (x,t)$, where $x \in \{0, \ldots, M-1\}$ denotes the position of the site in the horizontal axis and $t \in \{0, 1, \ldots, L-1\}$ denotes the position in the vertical axis. The t-coordinate is also known as the time coordinate since it starts at $t = 0$ from the top row and increases as an avalanche develops down

the lattice through time (Fig. 5.2). By definition the cylindrical lattice assumes periodic boundary conditions and thus the x-coordinate can be written in modulo M.

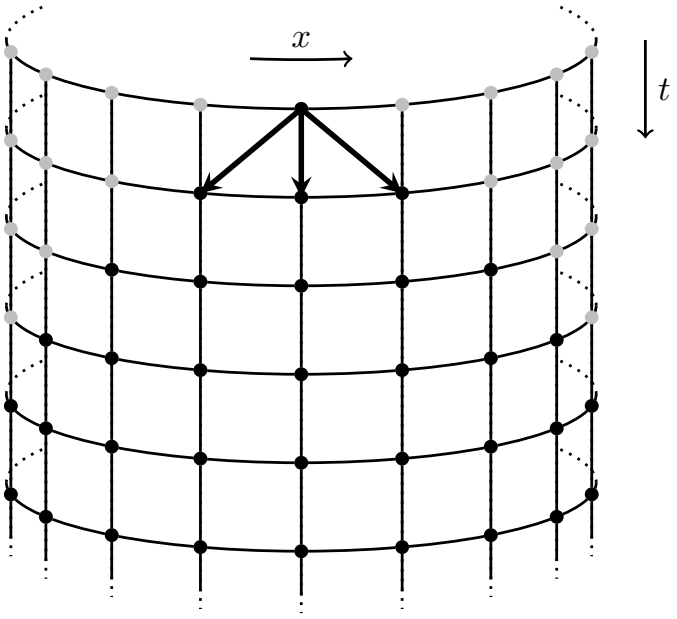


Figure 5.2 **Illustration of the directed sandpile model on a cylindrical lattice.** Each site has $K = 3$ downward neighbours and is allowed to have a height of $h(x,t) = 0,1,2$, where $t = 0,1,...,L-1$ and $x = 0,1,...,M-1$. When the height exceeds 2, then the site is said to topple and one particle is transferred to each of its $K = 3$ downward neighbours as denoted by the arrows. The light cone of the top site, the seed node, is indicated with sites having black circles; sites in grey will be unaffected by any avalanche initiated at that specific seed.

The variable of interest for each site is the height of the pile, $h(x,t) \in \mathbb{N}$ [1] defined as the number of particles each site $\vec{X} \equiv (x,t)$ is allowed to hold before it topples. For $h(x,t) < K$ the site is stable and can hold onto the particles it has. But for $h(x,t) \geq K$, the site is said to be unstable and thus it topples by giving one particle to each of its downward neighbours. For example, in the $K = 3$ system shown in Fig. 5.2, any toppling site (x,t) will relax by giving one particle to each of its three downward neighbours: $(x-1,t+1),(x,t+1)$ and

[1] The natural numbers here are all non-negative integers including zero, i.e. $\mathbb{N} = \{|a| : a \in \mathbb{Z}\}$.

$(x+1,t+1)$.

The directed sandpile model is said to be Abelian, since the order by which a couple of particles are added to different sites is irrelevant to the final state of the configuration, when all avalanches have terminated. In other words, driving the system from site (x_1,t) and then (x_2,t) makes no difference to the final heights of all sites had the system been driven in the reverse order [24].

If the system is allowed to be driven from any sites, then clearly in the steady state there exist K^{LM} different configurations that can occur with equal probability [25]. If the addition of particles is restricted to the top row only, then we get K^{L-1} disjoint sectors, tracing the light cone of the driving site. However, the avalanche statistics of the steady state in the thermodynamic limit where $L,M \gg 1$, are completely independent of the sector.

Without loss of generality, assume that the system is driven from the top layer $t = 0$ and so particles are randomly added to seed sites, one at a time. As the configuration relaxes, sites topple and an avalanche propagates through the lattice. In the case where the avalanche reaches the bottom layer $t = L-1$ and causes a toppling there, the three associated particles of the site are removed from the system. The avalanche cluster is the collection of sites that toppled after adding a single particle to the seed node and avalanche size s is defined as the total number of topplings that occurred in the cluster.

5.3 Calculation of the 2-point correlation function

Assume that our sandpile has reached an equilibrium state and now drive the system at $\vec{O} \equiv (0,0)$, the origin.

Then, the 2-point correlation function $G_2(x,t)$ is defined as the expected number of topplings at $\vec{X}$, that were caused by $\vec{O}$ toppling after driving the system at $\vec{O}$, i.e.,

$$G_2(x,t) = \langle \eta(\vec{X}) \rangle, \tag{5.1}$$

where $\eta(\vec{X})$ denotes the variable that indicates whether driving the system at $\vec{O}$ caused a toppling at the site $\vec{X} \equiv (x,t)$.

By definition, $G_2(0,0) = 1$, since this is estimating the expected number of topplings at the origin under the condition that the origin topples.

In the case where $K = 3$, once the system is out of the transient and has reached a steady state, all sites $\vec{X} = (x,t)$ have an equal probability of being height $h(x,t) = 0,1,2$. Therefore, the expected probability that (x,t) topples in a single avalanche is nothing more than the normalised sum of probabilities of the (x,t) upward neighbours have toppled. It is normalised by $1/3$ since (x,t) only takes one out of the three particles that its upward neighbour transfers upon toppling.

In other words, $G_2(x,t)$ satisfies the following equation:

$$G_2(x,t) = \frac{1}{3}\left(G_2(x-1,t-1) + G_2(x,t-1) + G_2(x+1,t-1)\right),$$

$$= \frac{1}{3}\sum_{\delta=-1}^{1} G_2(x+\delta,t-1). \tag{5.2}$$

Using the boundary condition $G_2(x,t=0) = \delta_{x,0}$, where $\delta_{x,0} = 1$ if x is the driving site and zero otherwise, Eq. (5.2) can be used to determine the 2-point correlation function $\forall x,t$.

The function $G_2(x,t=0)$ can be determined by first determining the associated characteristic function and then taking the inverse. The characteristic function $\tilde{G}_2(k,t)$ is defined as:

$$\tilde{G}_2(k,t) = \sum_x G_2(x,t)e^{ikx}. \tag{5.3}$$

Opening the sum using Eq. (5.2) and gathering terms, yields:

$$\tilde{G}_2(k,t) = \sum_x G_2(x,t)e^{ikx}$$

$$= \frac{1}{3}\sum_x \left(G_2(x-1,t-1) + G_2(x,t-1) + G_2(x+1,t-1)\right)e^{ikx}$$

$$= \frac{1}{3}\Big(\sum_x G_2(x-1,t-1)e^{ik(x-1)}e^{ik} + \sum_x G_2(x,t-1)e^{ikx} + \sum_x G_2(x+1,t-1)e^{ik(x+1)}e^{-ik}\Big)$$

$$= \frac{1}{3}(e^{ik} + 1 + e^{-ik})\tilde{G}_2(k,t-1)$$

$$= \frac{1}{3}(1 + 2\cos k)\tilde{G}_2(k,t-1). \tag{5.4}$$

Note that Eq. (5.4) is a recursive relationship that can be expanded from $t-1$ until 0 as follows:

$$\begin{aligned}
\tilde{G}_2(k,t) &= \frac{1}{3}(1+2\cos k)\tilde{G}_2(k,t-1) \\
&= \frac{1}{3}(1+2\cos k)(1+2\cos k)\tilde{G}_2(k,t-2) \\
&\quad \vdots \\
&= \frac{1}{3}(1+2\cos k)(1+2\cos k)^{(t-1)}\tilde{G}_2(k,0) \\
&= \frac{1}{3}(1+2\cos k)^t, \qquad (5.5)
\end{aligned}$$

where $\tilde{G}_2(k,0) = 0$ on use of the boundary condition $G_2(x,t=0) = \delta_{x,0}$ and Eq. (5.3).

Taking the inverse transform of Eq. (5.3) gives

$$G_2(x,t) = \int_0^{2\pi} \frac{dk}{2\pi} \tilde{G}_2(k,t) e^{-ikx} \qquad (5.6)$$

and substituting the above form for $\tilde{G}_2(k,t)$ from Eq. (5.4) yields:

$$G_2(x,t) = \int_0^{2\pi} \frac{dk}{2\pi} \left[\frac{1+2\cos k}{3}\right]^t e^{-ikx}. \qquad (5.7)$$

From here, it is easy to see that $G_2(x,t)$ vanishes strictly for all $|x| > t$ and that the region traced by $|x| \leq t$ is what is called the future light cone (see Fig. 5.2) of the driving site, the origin in this case. Also, for $t \gg 1$, $G_2(x,t)$ can be approximated by a Gaussian with mean

zero and variance $2t/3$.

The number of topplings in each layer that were a direct cause of the driving at $\vec{O}$ are defined as $\Phi(t)$, where

$$\Phi(t) = \sum_x \eta(x,t). \tag{5.8}$$

One can deduce that in the steady state

$$\langle \Phi(t) \rangle = \sum_x G_2(x,t) = 1, \text{ for all } t, \tag{5.9}$$

since the mean flux out of a layer equals the rate at which particles are added at the origin.

Then, the mean square flux $\langle \Phi^2(t) \rangle$ is by definition:

$$\langle \Phi^2(t) \rangle = \sum_{x_1,x_2} \langle \eta(x_1,t)\eta(x_2,t) \rangle. \tag{5.10}$$

However, denoting $G_3(x_1,x_2|t)$as

$$G_3(x_1,x_2|t) = \langle \eta(x_1,t)\eta(x_2,t) \rangle \tag{5.11}$$

yields

$$\langle \Phi^2(t) \rangle = \sum_{x_1,x_2} G_3(x_1,x_2|t). \tag{5.12}$$

Note, that since each site $\vec{X}$ topples at most once, $G_3(x_1,x_2|t)$ is just the probability that

both, site $\vec{X}_1$ and site $\vec{X}_2$ have toppled in a given avalanche.

5.4 Calculation of the 3-point correlation function

Let us take two sites in layer t, namely (x_1,t) and (x_2,t), and define $(x_1+\delta_1,t-1)$ and $(x_2+\delta_2,t-1)$ where $\delta_1,\delta_2 \in \{-1,0,1\}$ to be their respective upward neighbours. For the case where $x_1 \neq x_2$, since (x_1,t) and (x_2,t) have three upward neighbours each, then the probability that they topple equals to a third of the number of topplings of their neighbours, i.e.,

$$\tilde{G}_3(x_1,x_2|t) = \sum_{\delta_1,\delta_2=-1}^{+1} \left\langle \frac{1}{3}\eta(x_1+\delta_1,t-1)\frac{1}{3}\eta(x_2+\delta_2,t-1) \right\rangle$$

$$= \frac{1}{9}\sum_{\delta_1,\delta_2=-1}^{+1} \langle \eta(x_1+\delta_1,t-1)\eta(x_2+\delta_2,t-1)\rangle. \tag{5.13}$$

Using the definition of $G_3(x_1,x_2|t)$ from Eq. (5.11) we have that for all $x_1 \neq x_2$:

$$G_3(x_1,x_2|t) = \frac{1}{9}\sum_{\delta_1,\delta_2=-1}^{+1} G_3(x_1+\delta_1,x_2+\delta_2|t-1). \tag{5.14}$$

From this, we can clearly see that $G_3(x_1,x_2|t)$ is the expected product of the number of times (x_1,t) and (x_2,t) topple.

In the special case where $x_1 = x_2$, the relation of the toppling indicator $\eta(x_1+\delta_1, t-1)\eta(x_2+\delta_2, t-1)$ reduces to $\eta^2(x_1,t) = \eta(x_1,t)$. Thus, from Eq. (5.13) we have that

$$G_3(x_1,x_1|t) = G_2(x_1,t) \quad \forall x_1. \tag{5.15}$$

Now, let $G_2[\vec{X}|\vec{Y}]$ denote the expected number of topplings at site $\vec{X} = (x,t)$, from an avalanche generated by a particle addition at site $\vec{Y} = (y,t')$. For a particle added at the origin, it is easy to verify that Eq. (5.13) is satisfied for

$$G_3(x_1,x_2|t) = G_2[\vec{X}_1|\vec{O}]\; G_2[\vec{X}_2|\vec{O}]. \tag{5.16}$$

Clearly,

$$G_2[\vec{X}|\vec{Y}] = G_2(\vec{X}-\vec{Y}) = G_2(x-y, t-t'), \tag{5.17}$$

and the function $G_2[\vec{X}|\vec{Y}]$ inherits the light-cone structure of $G_2(x,t)$, where it is nonzero if and only if $\vec{X}$ is in the future-light cone of $\vec{Y}$.

To seek a solution that is consistent with the boundary conditions Eq. (5.15) for when $x_1 = x_2$, consider the following superposition of such solutions [26]:

$$G_3(x_1,x_2|t) = \sum_{\vec{Y}} f(\vec{Y}) G_2[\vec{X}_1|\vec{Y}] G_2[\vec{X}_2|\vec{Y}]. \tag{5.18}$$

The summation over $\vec{Y}$ looks like it extends over all sites, but technically due to the light-cone structure of the propagator G_2, only sites that sit in the intersection of the future light-cone of $\vec{O}$ with the past light-cones of both $\vec{X}_1$ and $\vec{X}_2$ can actually make a contribution to the sum.

For this solution, the boundary conditions outlined in Eq. (5.15) that can be used to determine the unknown coefficients $f(\vec{Y})$ take the form

$$G_2(\vec{X}) = \sum_{\vec{Y}} f(\vec{Y}) G_2^2[\vec{X}|\vec{Y}], \quad \forall \vec{X}, \tag{5.19}$$

where we assumed that $\vec{X}_1 = \vec{X}_2 = \vec{X}$ and that the summation over $\vec{Y}$ is in fact over all sites that sit in the future light-cone of the origin and the backward light-cone of $\vec{X}$.

If one wishes to determine the unknown function $f(\vec{Y})$, then this can be done by starting from the driving site and recursively using the above set of coupled linear equations for sites $\vec{Y}$ in the past-light cone of $\vec{X}$. However, one does not need to know all the values of $f(\vec{Y})$s for all $\vec{Y}$ as we are only using their sum a each time layer t. So let us denote this sum, for all times $t \geq 0$, as

$$F(t) = \sum_{x} f((x,t)). \tag{5.20}$$

Now, substituting our general solution (Eq. (5.18)) into our expression for $\langle \Phi^2(t) \rangle$ as shown in Eq. (5.12) yields:

$$\langle \Phi^2(t) \rangle = \sum_{x_1,x_2} \sum_{\vec{Y}} f(\vec{Y}) G_2[\vec{X}_1|\vec{Y}] G_2[\vec{X}_2|\vec{Y}]. \tag{5.21}$$

Doing summations over x_1, x_2 and t', using Eq. (5.9), and Eq. (5.20), we get

$$\langle \Phi^2(t) \rangle = \sum_{t'=0}^{t} F(t'). \tag{5.22}$$

Let us define the function $K(t)$ which vanishes with $G_2(x,t)$ for $t < 0$:

$$K(t) = \sum_x G_2^2(x,t). \tag{5.23}$$

Summing over all sites $\vec{X}$ in layer t on both sides of Eq. (5.19) and using Eq. (5.20)gives:

$$\begin{aligned}
\sum_x G_2(x,t) &= \sum_{y,t} f(y,t') \sum_x G_2^2(x-y,t-t') \\
&= \sum_{y,t} f(y,t') K(t-t') \\
&= \sum_t \sum_y f(y,t') K(t-t') \\
&= \sum_t F(t') K(t-t'). \qquad (5.24)
\end{aligned}$$

On use of Eq. (5.9) this reduces to:

$$1 = \sum_{t'=0}^{t} F(t') K(t-t'). \tag{5.25}$$

Here, it is worth noting that Eq. (5.25) has an extra factor in comparison to its analogous one in Dhar *et al.* [26], which is due a different normalisation of $G_2(\vec{X})$. Also, without loss of generality and since $K(t-t')$ vanishes with $t < t'$, the summation over t' is extended to $+\infty$:

$$1 = \sum_{t'=0}^{\infty} F(t') K(t-t'). \tag{5.26}$$

Hence, we can define the generating functions of $F(z)$ and $K(z)$ as follows:

$$\tilde{F}(z) = \sum_{t=0}^{\infty} F(t) z^t \tag{5.27a}$$

$$\tilde{K}(z) = \sum_{t=0}^{\infty} K(t) z^t \tag{5.27b}$$

and use these to express Eq. (5.26) in a different form:

$$\begin{aligned}
\sum_{t=0}^{\infty} 1 \cdot z^t &= \sum_{t=0}^{\infty} \sum_{t'=0}^{\infty} F(t') K(t-t') z^t \\
&= \sum_{t'=0}^{\infty} F(t') z^{t'} \sum_{t=0}^{\infty} K(t-t') z^{t-t'} \\
&= \sum_{t'=0}^{\infty} F(t') z^{t'} \sum_{t''=0}^{\infty} K(t'') z^{t''} \\
&= \tilde{F}(z) \tilde{K}(z)
\end{aligned} \tag{5.28}$$

where we defined $t'' = t - t'$ and $K(t'') = 0$ for all $t'' < 0$. Note, that the left hand side of the above equation is just a geometric sum, so Eq. (5.28) reduces to:

$$\frac{1}{1-z} = \tilde{F}(z) \tilde{K}(z). \tag{5.29}$$

During a given avalanche, any site $\vec{X}' = (x', t')$ can topple a maximum of one time, thus its

expected number of topplings is equal to the probability for it to topple. We have already defined $G_2(x,t)$ to be the expected number of topplings at site $\vec{X}$ given that when the system was driven at the origin $\vec{O}$ it launched an avalanche. We also know that due to the Abelian property of the system the total number of topplings at another site $\vec{X'} = (x',t')$, which is in the light cone of $\vec{X} = (x,t)$, is the sum of all the topplings triggered by the event of $\vec{X}$ toppling. This allows us to define the expected number of topplings at site $\vec{X'}$ given that when the system was driven by the toppling of another site $\vec{X} = (x,t)$, which is in the past light cone of $\vec{X'}$ as:

$$G_2[\vec{X'}] = \sum_x G_2[\vec{X}] G_0[\vec{X'}|\vec{X}] \tag{5.30}$$

which is equivalent to

$$G_2(x',t') = \sum_x G_2(x,t) G_2(x'-x,t'-t) \tag{5.31}$$

where the notation was just changed and $0 \leq t \leq t'$.

From this, we can express the expected number of topplings at site $(0,2t)$ in the following form:

$$\begin{aligned} G_2(0,2t) &= \sum_x G_2(x,t) G_2(0-x,2t-t) \\ &= \sum_x G_2(x,t) G_2(-x,t) \\ &= \sum_x G_2^2(x,t). \end{aligned} \tag{5.32}$$

On use of Eq. (5.23) this reduces to:

$$G_2(0,2t) = K(t). \tag{5.33}$$

Substituting this in the generating function in Eq. (5.27b) yields:

$$\tilde{K}(z) = \sum_{m=0}^{\infty} G_2(x=0,t=2m)z^m, \tag{5.34}$$

with t only taking even values.

Now, let us define $H(z)$, such that:

$$H(z) = \sum_{m=0}^{\infty} G_2(0,m)z^m. \tag{5.35}$$

Then, by definition

$$H(z)+H(-z) = \sum_{m=0}^{\infty} G_2(0,m)z^m + \sum_{m=0}^{\infty} G_2(0,m)(-z)^m$$

$$= 2\sum_{m=0}^{\infty} G_2(0,2m)z^{2m} \tag{5.36}$$

since all the odd terms cancel. This implies that,

$$H(\sqrt{z})+H(-\sqrt{z}) = 2\sum_{m=0}^{\infty} G_2(0,2m)z^m. \tag{5.37}$$

We can substitute this expression into Eq. (5.34), our equation for $\tilde{K}(z)$ as the sum only

includes even values of t in $G_2(0,t)$:

$$\tilde{K}(z) = \frac{1}{2}[H(\sqrt{z}) + H(-\sqrt{z})]. \tag{5.38}$$

We can evaluate this further by going back to our definition of $H(z)$. Substituting Eq. (5.7) with $x = 0$ and $t = m$ into Eq. (5.35) yields

$$\begin{aligned} H(z) &= \sum_{m=0}^{\infty} \int_0^{2\pi} \frac{dk}{2\pi} \left[\frac{1+2\cos k}{3}\right]^m z^m \\ &= \int_0^{2\pi} \frac{dk}{2\pi} \sum_{m=0}^{\infty} \left[\frac{z(1+2\cos k)}{3}\right]^m \\ &= \int_0^{2\pi} \frac{dk}{2\pi} \frac{3}{3 - z(1+2\cos k)} \end{aligned} \tag{5.39}$$

where the known result of the geometric sum $\sum_{k=0}^{\infty} r^k = \frac{1}{1-r}$ was utilised. The above expression can be rearranged to allow for integration using well known general integrals as

follows:

$$
\begin{aligned}
H(z) &= \frac{3}{4\pi z}\int_0^{2\pi} dk\ \frac{1}{\left(\frac{3-z}{2z}\right)-\cos k} \\
&= \frac{3}{2\pi z}\int_0^{\pi} dy\ \frac{1}{\left(\frac{3-z}{2z}\right)-\cos 2y} \\
&= \frac{3}{2\pi z}\int_0^{\pi} dy\ \frac{1}{\left(\frac{3-z}{2z}\right)-\left(\frac{1-tan^2y}{sec^2y}\right)} \\
&= \frac{3}{2\pi z}\int_0^{\pi} dy\ \frac{sec^2y}{\left(\frac{3-z}{2z}\right)sec^2y-1+tan^2y} \\
&= \frac{3}{2\pi z}\int_0^{\pi} dy\ \frac{sec^2y}{\left(\frac{3-z}{2z}\right)(tan^2y+1)-1+tan^2y} \\
&= \frac{3}{2\pi z}\int_0^{\pi} dy\ \frac{sec^2y}{\left(\left(\frac{3-z}{2z}\right)-1\right)+\left(\left(\frac{3-z}{2z}\right)+1\right)tan^2y} \\
&= \frac{3}{2\pi z}\int_{-\infty}^{\infty} \frac{dt}{sec^2y}\ \frac{sec^2y}{\left(\left(\frac{3-z}{2z}\right)-1\right)+\left(\left(\frac{3-z}{2z}\right)+1\right)t^2} \\
&= \frac{3}{2\pi z}\int_{-\infty}^{\infty} dt\ \frac{1}{\left(\left(\frac{3-z}{2z}\right)-1\right)+\left(\left(\frac{3-z}{2z}\right)+1\right)t^2} \\
&= \frac{3}{2\pi z\left(\left(\frac{3-z}{2z}\right)+1\right)}\int_{-\infty}^{\infty} dt\ \frac{1}{\left(\frac{\left(\frac{3-z}{2z}\right)-1}{\left(\frac{3-z}{2z}\right)+1}\right)+t^2}.
\end{aligned}
\tag{5.40}
$$

Finally, evaluating the integral over the limits yields:

$$H(z) = \frac{3}{2\pi z\left(\left(\frac{3-z}{2z}\right)+1\right)}\left(\frac{\left(\frac{3-z}{2z}\right)+1}{\left(\frac{3-z}{2z}\right)-1}\right)^{\frac{1}{2}}\left[tan^{-1}\frac{t}{\left(\frac{\left(\frac{3-z}{2z}\right)-1}{\left(\frac{3-z}{2z}\right)+1}\right)^{\frac{1}{2}}}\right]_{-\infty}^{\infty}$$

$$= \frac{3}{2\pi z\left(\left(\frac{3-z}{2z}\right)+1\right)}\left(\frac{\left(\frac{3-z}{2z}\right)+1}{\left(\frac{3-z}{2z}\right)-1}\right)^{\frac{1}{2}}\pi$$

$$= \frac{3}{2z\sqrt{\left(\left(\frac{3-z}{2z}\right)+1\right)\left(\left(\frac{3-z}{2z}\right)-1\right)}}$$

$$= \frac{3}{2z\sqrt{\left(\frac{3-z}{2z}\right)^2-1}}$$

$$= \frac{3}{\sqrt{(3-z)^2-4z^2}}$$

$$= \frac{3}{\sqrt{9-6z-3z^2}}$$

$$= \frac{3}{\sqrt{3(3-2z-z^2)}}$$

$$= \frac{\sqrt{3}}{\sqrt{(1-z)(3+z)}}. \tag{5.41}$$

Substituting this into Eq. (5.38) yields:

$$\tilde{K}(z) = \frac{1}{2}\left(\frac{\sqrt{3}}{\sqrt{(1-\sqrt{z})(3+\sqrt{z})}} + \frac{\sqrt{3}}{\sqrt{(1+\sqrt{z})(3-\sqrt{z})}}\right)$$

$$= \frac{\sqrt{3}}{2}\frac{\sqrt{(1+\sqrt{z})(3-\sqrt{z})} + \sqrt{(1-\sqrt{z})(3+\sqrt{z})}}{\sqrt{(1-z)(9-z)}}. \tag{5.42}$$

This expression for $\tilde{K}(z)$ can be substituted into Eq. (5.29) to get an explicit function $\tilde{F}(z)$ in terms of z:

$$\tilde{F}(z) = \frac{1}{(1-z)\tilde{K}(z)} \tag{5.43}$$

$$= \frac{2}{\sqrt{3}}\frac{1}{(1-z)}\frac{\sqrt{(1-z)}\sqrt{(9-z)}}{\sqrt{(1+\sqrt{z})(3-\sqrt{z})} + \sqrt{(1-\sqrt{z})(3+\sqrt{z})}}$$

$$= \frac{2}{\sqrt{3}}\frac{1}{\sqrt{(1-z)}}\frac{\sqrt{(9-z)}}{\sqrt{(1+\sqrt{z})(3-\sqrt{z})} + \sqrt{(1-\sqrt{z})(3+\sqrt{z})}}. \tag{5.44}$$

It is clear from Eq. (5.42) that $\tilde{K}(z)$ has a dominant singularity for z in the vicinity 1 of the form $(1-z)^{-1/2}$, where z is tending to 1 from below. The same leading behaviour is evident from Eq. (5.43) for $\tilde{F}(z)$.

Hence $F(t)$ varies as $t^{-1/2}$ for large t and then $\langle \Phi^2(t) \rangle$ varies as $t^{1/2}$.

This is consistent with the behaviour found by Dhar and Ramaswamy [26] for the case with coordination number $K = 2$. The probability that $\Phi(t) \neq 0$ decreases like $t^{-1/2}$ for large t, but once it is non-zero, its typical value is of order $t^{+1/2}$ consistent with the mean value of 1 (see Eq. (5.9)). Then, for large t, the mean value $\langle \Phi^2(t) \rangle$ will to grow as $t^{1/2}$.

5.5 Corrections to scaling

Avalanches on regular lattices with co-ordination number $K = 2$ are compact, whereas for $K > 2$ they branch out, as observed in Fig. 5.1. The structural changes in avalanches mean that the argument for compact avalanches and two annihilating random walkers may no longer be valid as the obvious side branches have created holes in the developing avalanches.

There seems to be a deviation to scaling for $K = 3$, but this is slowly converging which suggests that perhaps the structural differences in the underlying topology for $K = 3$ compared to $K = 2$, *i.e.* the appearance of side-branches and holes, may be irrelevant if one corrects for the fact that the system is now running into strong finite size effects.

One can Taylor expand $\tilde{F}(z)$ as a series of z by using Eqs. (5.29) and (5.42) and thus determine the exact values of $\langle \Phi^2(t) \rangle$. The main plot in Fig. 5.3 shows the exact values of $\langle \Phi^2(t) \rangle$ for $1 \leq t \leq 1000$, where a simple fit of the power-law yields:

$$\langle \Phi^2(t) \rangle \approx a t^{\alpha} \tag{5.45}$$

with $a \approx 1.61$ and $\alpha \approx 0.52$.

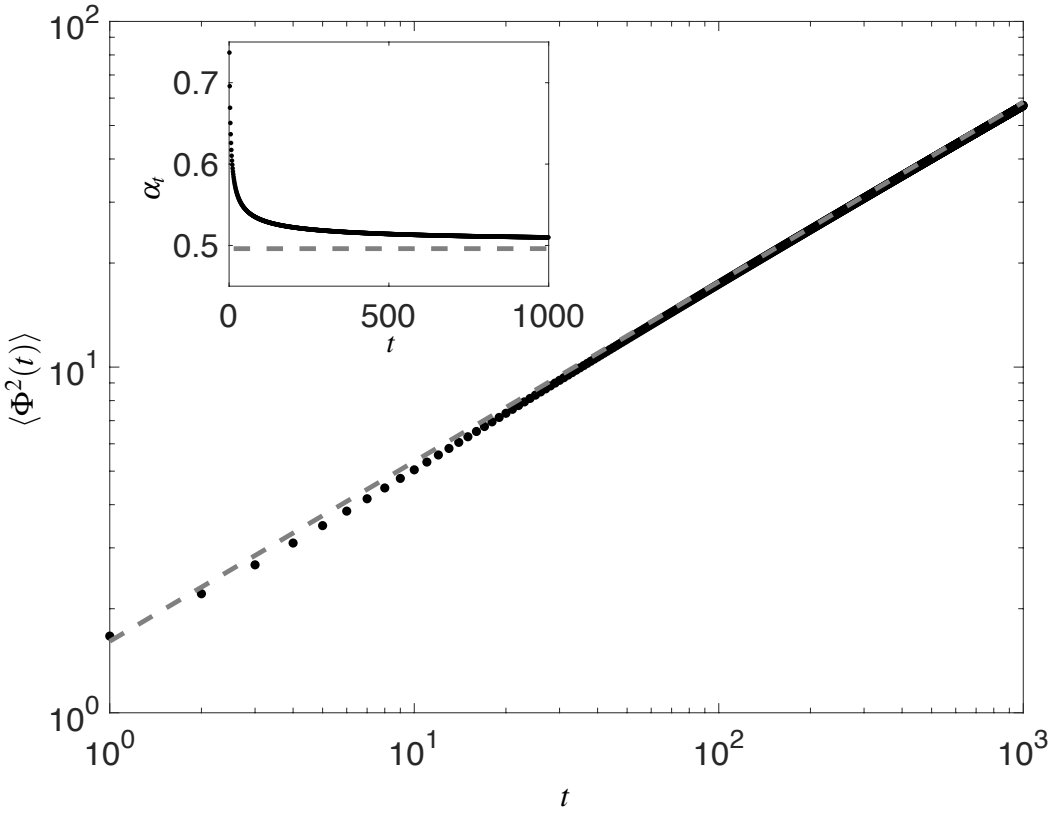


Figure 5.3 **Corrections to scaling.** The main figure shows the behavior of the mean squared flux $\langle \Phi^2(t) \rangle$ as a function of the depth t, $1 \leq t \leq 1000$, determined from the exact series expansion of $\tilde{F}(z)$ (black dotted line) in a double-logarithmic plot. The best visual fit to the function $f(t) = at^{\alpha}$ given by the estimated parameters $a \approx 1.61, \alpha \approx 0.52$ (grey dashed line). In the inset, we plot effective exponent α_t, defined in Eq. (5.47) (black dotted line) which slowly converges to the exact value 0.5 (grey dashed line), as $\langle \Phi^2(t) \rangle \propto t^{1/2}$. Both plots in this figure show that corrections to scaling are still large for avalanches of duration of order 10^3, that is, avalanches that reach $t = 1000$.

Using Eq. (5.45) for t and $t+1$ to eliminate a allows us to get an expression in terms of α_t and t, only:

$$\frac{\langle \Phi^2(t) \rangle}{t^{\alpha}} \approx \frac{\langle \Phi^2(t+1) \rangle}{(t+1)^{\alpha}}. \tag{5.46}$$

After some trivial rearranging and taking logarithms of both sides this yields:

$$\alpha_t \approx \frac{\log\left(\langle\Phi^2(t+1)\rangle/\langle\Phi^2(t)\rangle\right)}{\log\left((t+1)/t\right)}, \tag{5.47}$$

which can be used to plot the effective exponent α_t as illustrated in the subplot of Fig. (5.3) for the values $1 \leq t \leq 1000$. From this, it is clear that the effective exponent α_t is converging, albeit very slowly, to the value 0.5. These two plots taken together illustrate how large the corrections to scaling actually are and the importance of taking these into account when estimating exponents from numerical data.

On the other hand, knowing that $\langle\Phi^2(t)\rangle$ is proportional to $t^{1/2}$ means that the probability that an avalanche duration is greater than t tends to $t^{-1/2}$. This implies that the avalanche duration exponent is $3/2$ is equivalent to the avalanche dimension D in a directed model, i.e. $D = 3/2$ (see Sec. 8.4.3 in Pruessner (2012) [72]). The other exponents follow from this and are exactly the same as the case with coordination number $K = 2$ [26].

Pinho and Andrade [69] conducted similar analysis for a directed sandpile model of rainfall where the critical height is $h = 4$ and a toppling at (x,t) caused one particle to be transferred to $(x-1,t+1)$ and $(x+1,t+1)$ each and two particles to $(x,t+1)$. The two-point correlation function $G_2(x,t)$ was calculated exactly but the functions $K(t)$ and $F(t)$ were estimated recursively numerically for small t and again large corrections to scaling were found. Unlike here, no explicit analytical expressions for $F(t)$ or $K(t)$ were determined.

5.6 Numerical simulations

Large scale numerical simulations were implemented in order to provide reliable numerical estimates of the critical exponents. In the following section the issues arising from these, the fitting models used and finally the critical exponent estimates found are discussed in more detail.

5.6.1 Initialisation

The directed sandpile is a deterministic model, with the only stochasticity arising at the driving, when a new sand grain is added onto a randomly chosen node in the first layer. Moreover, this stochasticity is apparent since the order by which the nodes in the first layer are chosen is irrelevant since the model is Abelian [24]. Every state is recurrent and thus one may start from an empty lattice with $h(x,t) = 0$ as this configuration can indeed be present at the stationary state. Once a toppling occurs it sends K particles downstream and every particle that is added at the top performs L moves to move through all the layers in the system before exiting in the final row. Therefore, K particle additions will cause L number of topplings in KL moves and thus the average number of topplings that occur in the system after dropping a particle in the top row is

$$\langle s \rangle = L/K, \tag{5.48}$$

where s is known as the avalanche size. Note that this definition includes avalanches of size zero.

When initialising the system from an an empty lattice configuration, the first moment of the avalanche cluster size s in a system where $K = 4$, $L = 512$ and the circumference $M = 3072$ shows very good convergence within $2 \cdot 10^7$ driving events in the top row layer. However, the second moment still doesn't converge after $5 \cdot 10^{10}$ avalanche events and higher moments need even longer transients as they are even more noisy. This confirms that once the system has reached a *steady state*, where there are no spacial correlations, the temporal correlations are still present albeit decaying very slowly.

Initialising the lattice randomly with independent uniformly distributed heights $h(x,t) < K$ reduces the transient times drastically but still generates the same moment estimates as starting from an empty configuration and taking estimates after the very long transients. The empty state, although recurrent, is not a typical one and thus initialising the system from this requires a very long time before the correlations, caused by this unique state, vanish. However, in a random recurrent state the transient avalanche size moments estimates no longer drifted within a minimal transient time.

5.6.2 Parameters and Results

In the results that follow, different system sizes and coordination numbers were tested: $K = 2,3,4$, $L = 2^r$, with r taking integer values from 4 to 14 and with chosen width $M \geq L(K-1)$ so that even the largest avalanche possible would not topple all sites in a single layer. As in all the simulations presented thus far, the Mersenne Twister pseudo-random number generator [52] was used to (a) randomly initialise the lattice, and (b) choose which site in the top row to add a particle on in order to drive the system.

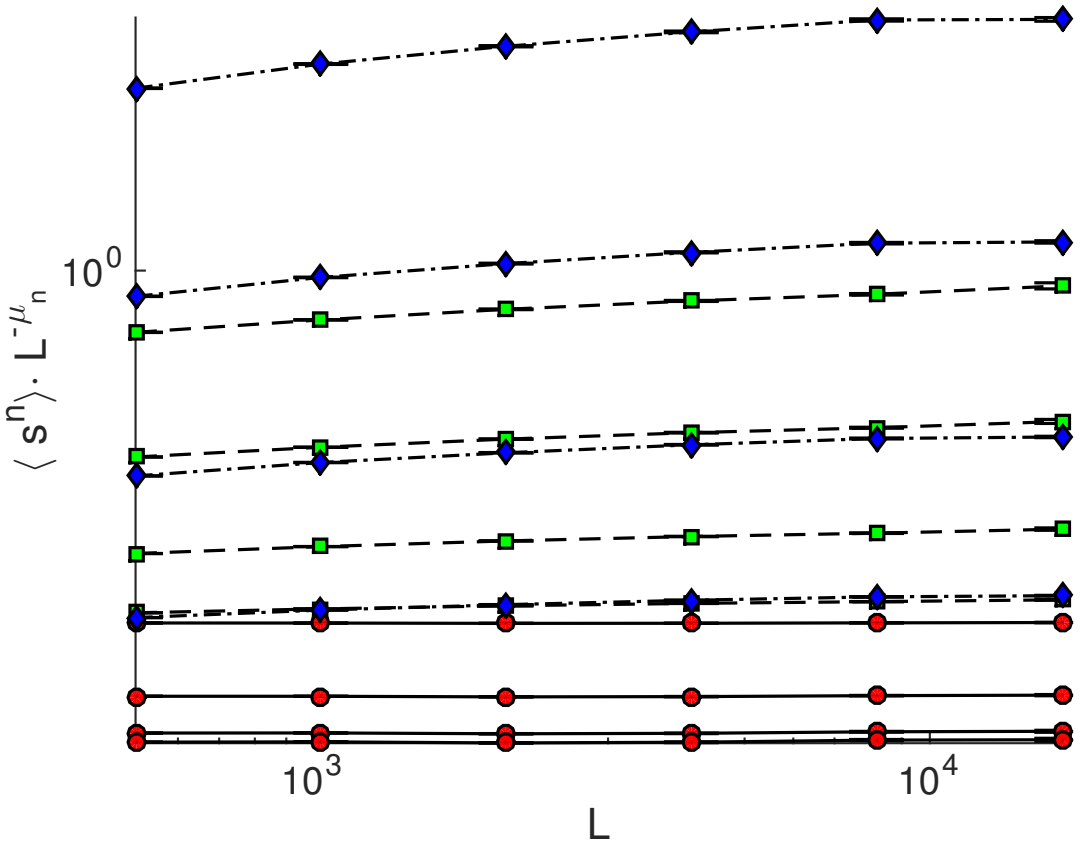


Figure 5.4 **Moments analysis.** The scaled moments $\langle s^n \rangle L^{-\mu_n}$ plotted against the height of the lattice L for $n = 2,3,4,5$. The data shown is for different $K = 2$ (red circles), $K = 3$ (green squares) and $K = 4$ (blue diamonds). For the same K, a higher curve corresponds to higher n. Note that for increasing K, the corrections to scaling become more important.

The avalanche sizes were recorded and used to calculate the moments $\langle s^n \rangle$ for $n = 2$ to 5.

The moments $\langle s^n \rangle$ are expected to scale with L^{μ_n}, $\mu_n = D(1 - \tau + n)$ see Eq. (4.9). Hence, in Fig. 5.4, the scaled moments $\langle s^n \rangle L^{-\mu_n}$ are plotted against height of the lattice L in oder to expose any corrections to scaling.

Statistical errors were estimated by measuring the variance of 10^6 avalanches at a time,

where at least several thousand of these chunks were used for each system configuration. Merging independent chunks of avalanches together should not cause a change in the variance, and thus this was used as a control to merge these together until no change was observed alluding to the fact that chunk had become independent. Once at this stage, one can use the now independent measurements to estimate the statistical errors of the mean of a moment by finding the estimated standard deviation of the moments across all chunks and divide this by the square root of the number of independent chunks.

Extremely large events are rare, but still exist, and when they occur they contribute a great weight to the moments whose relative error is proportional to their order. For example, in the simulations for $K = 3$ and $L = 16384$ that included $3.8 \cdot 10^8$ avalanche events, the error for the second moment was approximately 0.00016 whereas for the eighth moment it increased to 0.014. In Fig. 5.4 one can see the results for moments up to order 5.

Performing finite-size scaling of the probability density function (pdf) of the avalanche sizes s shows that the moments scale with the system size L according to the following relation [72]:

$$\langle s^n \rangle = a_n L^{\mu_n} \quad \text{for } L \gg 1, \tag{5.49}$$

where a_n are metric factors that do not depend on L and $\mu_n = D(1 - \tau + n)$.

The avalanche size exponent is $\tau \geq 1$ and D is known as the fractal dimension of avalanche clusters [17]. Both critical exponents τ and D are expected to be universal, *i.e.*, they are independent of L, but they are not independent of each other since $\langle s \rangle = L/K$ and thus by Eq. (5.48) the following relation holds true $D(2 - \tau) = 1$, as observed across all the numerical simulations.

For τ strictly greater than 1, as is the case here, the variance of the nth moment can be derived from Eq. (5.49) like so:

$$\begin{aligned}\frac{\sqrt{\langle s^{2n}\rangle}}{\langle s^n\rangle} &= \frac{\sqrt{a_{2n}L^{D(1-\tau+2n)}}}{a_n L^{D(1-\tau+n)}} \\ &= \frac{\sqrt{a_{2n}}}{a_n}L^{D(1-\tau)/2} \\ &\propto L^{D(1-\tau)/2}\end{aligned} \tag{5.50}$$

for independent samples. Clearly, this expression is dominated by the scaling of the $2n$th moment, which implies that it grows independently of the order of n and scales with the system size. Therefore, to get accurate moments one must keep increasing the system sizes proportionally.

Unfortunately, the simulation time of each avalanche is directly proportional to the average avalanche size that scales linearly with system size L. However, larger system sizes have correlations that persist for a longer time, which means that getting independent samples in larger systems comes with increased costs in time.

Initialising the lattices randomly as discussed earlier, meant that the transient was very small and thus it was fairly easy to produce sufficient samples for the large systems sizes as well. In comparison, the samples for the smaller system sizes were very large, minimum 10^{10} per system tested. Very small system sizes, smaller than $L = 512$, need a large number of corrections to scaling terms which makes the analysis quite complicated. These were omitted from further calculations.

K	D	τ	D (ctos)	τ (ctos)
2	1.4999(11)	1.3333(05)		
3	1.5141(38)	1.3342(17)	1.5020(20)	1.3395(09)
4	1.5244(78)	1.3440(34)	1.4994(35)	1.3331(23)

Table 5.1 **Scaling exponents on regular lattices with corrections to scaling.** Numerical estimates of the avalanche dimension D, and the avalanche-size exponent τ that was derived from it via the scaling relation $\tau = 2 - 1/D$. The numerics for $K = 2$ were performed as a reference, as $D = 3/2$ and hence $\tau = 4/3$ was already known analytically [26]. The first two columns are fits without including corrections to scaling. The last two columns list the exponents extracted when the fit includes corrections to scaling (ctos) Eq. (5.52) for systems with $K = 3$ and 4. The errorbars listed in the brackets correspond to three standard deviations of the last two significant digits. When corrections to scaling are taken into account, the data is consistent with $D = 3/2$ and $\tau = 4/3$ for all K considered.

The critical exponent D, for each coordination number K, is extracted from moments' analysis. From Eq. (5.49), we have that for $L \gg 1$ the nth moment is proportional to L^{μ_n}, so plotting the moments $\langle s^n \rangle$ against system size L gives estimates for μ_n. However, from Eq. (5.49) we have that $\mu_n = D(1 - \tau + n)$ and we also have an expression for τ in terms of D from the scaling relation, which we can use to eliminate τ:

$$\begin{aligned} \mu_n &= D(1 - \tau + n) \\ &= D(1 - (2 - 1/D) + n) \\ &= 1 + D(n - 1). \end{aligned} \tag{5.51}$$

Therefore, by plotting μ_n against n one can easily extract the critical exponent D by simply looking at the gradient of the straight line. Following this, avalanche size exponent can be derived by simply substituting the values for D back into the scaling relation $\tau = 2 - 1/D$. The values for the critical exponents are reported in the first two column of Table 5.1. Note

here, that just like the exponents reported in the previous chapter, the critical exponents for $K = 2$ are consistent with the theoretical values for the two-dimensional directed sandpile universality class $\tau = 4/3$ and $D = 3/2$, but show significant deviation from the theoretical values for $K = 3$, which increases even more for $K = 4$. Clearly, performing large scale simulations reduced the observed drift in the exponents seen in Tab. 4.1, but did not eliminate it completely.

Corrections are needed for finite-size systems. Adding two corrections to scaling terms in the original fitting model yields a more accurate fitting model for finite-size

$$\langle s^n \rangle = a_n L^{\mu_n}(1 + b_n L^{-1/2} + c_n L^{-1}), \tag{5.52}$$

which can be used to fit each moment against system size L by using the Levenberg-Marquardt method [71]. Both corrections to scaling terms vanish as the system size tends to infinity.

In the instances where convergence was proving to be a problem, using fewer parameters provided an initial guess, which was used as an initial input. This was not ideal as normally this does not give the optimal fit, but needed in this case. If the resulting estimates for $n = 2$ up to 5 were within a 0.25 goodness of fit then they were accepted [71]. Also, from the first moment equation (see Eq. (5.48)) one can deduce that μ_1 must be unity. Thus, μ_n needs to be fitted linearly against $1 + D(n-1)$ only for $n = 2$ to 5.

The moments μ_n for $n = 2$ to 5 are obviously correlated amongst each other since they are all calculated from the same avalanche time series, but this is rather difficult to quantify. To go around this issue, the time series was cut into separate chunks and the estimates of μ_n were derived from *distinct* samples. The error of these was doubled to be on the safe side.

The estimates D and τ using the corrections to scaling (ctos) are reported in the last two columns of Tab. 5.1. Even though these seem to be extremely close the theoretical values of $D = 3/2$ and $\tau = 4/3$, it should be note that this was achieved using very large sample sizes, very large system sizes and quite long CPU time.

5.7 Summary

The directed sandpile model on a rigid regular lattice with coordination number $K = 2$, i.e. 2 downward neighbours per site, was solved analytically by Dhar and Ramaswamy [26], where it was shown that since the observed avalanches were compact, without any holes or side branches, the system is just an analogy for two annihilating random walkers.

However, for $K > 2$, this property no longer holds as obvious side branches create holes in the developing avalanches. This structural difference in avalanches led to the drift away from the avalanche size exponent $\tau = 4/3$ of the classical two-dimensional directed sandpile model universality class that was observed in the numerical simulations for the regular lattice with higher coordination number in Chapter 4 and [98].

Large scale Monte Carlo simulations with system sizes $L = 512, 1024, \ldots, 16384$, for $K = 2, 3, 4$ and subsequent moment analysis of these give numerical estimates for the critical exponents: the avalanche dimension D and τ on use of $\tau = 2 - 1/D$. As expected for $K = 2$, the numerical estimates are consistent with the exact result in [26], but for $K = 3$ and $K = 4$, the result again deviates from the avalanche dimension $D = 3/2$ and the avalanche size exponent $\tau = 4/3$. This is due to large scaling effects and, in fact, when these are corrected (see Eq. (5.52)) the numerical estimates for $K = 3$ and $K = 4$ become consistent with the

critical exponents for the directed sandpile model $K = 2$.

Moreover, the exponents for the $K = 3$ case are calculated analytically using a similar approach to the one in [26] and are identical to the $K = 2$ case. This confirms that the deviations from the $K = 2$ values observed in earlier simulations (see Table 4.1 on page 76) where $K > 2$ are due to corrections to scaling effects and that the critical exponents are consistent with the two-dimensional directed sandpile universality class for all coordination numbers $K \geq 2$.

Chapter 6

Avalanches in the real-world inter-firm network of the Japanese economy

Part of the material presented in this chapter was published in a peer-reviewed journal, where all contributing parties have been properly acknowledged [98]:
Zachariou, N., Expert, P., Takayasu, M., and Christensen, K. (2015). Generalised Sandpile Dynamics on Artificial and Real-World Directed Networks. PLoS ONE, 10(11):e0142685.

6.1 Introduction

For the convenience of the reader, a few points that were made in previous chapters are recapitulated here. Economists are keen to understand the observed instability to the economic aggregate that emerges from a constant demand because this is a highly costly problem, both

to the scheduling of production and to the management of inventory [77]. To investigate this problem in intersectoral trade, Bak *et al.* [7] redefined the classical two-dimensional directed sandpile model and applied it to the fluctuations of production. They recovered the scaling exponents of the classical universality class: $\tau = 4/3$ and $D = 3/2$, see Eq. (4.6).

In Chapter 4, the dynamics in a strictly layered $K = 2$ lattice [7, 26] were generalised to allow for a different number of producers and consumers, instead of only two, and the dynamics was run on a regular lattice network with increased coordination number $K \geq 2$. It was proven theoretically for $K = 3$ and shown numerically for $K = 3$ and 4 that strictly layered lattices with constant coordination number K remain in the classical universality class with $\tau = 4/3$ and $D = 3/2$ (see Chapter 5). However, the dynamics as defined in Section 4.2 can in fact be applied to even less rigid topologies and more realistic networks. By far the best real-world network for this task is the actual production-consumption network between all the firms in a real and active economy.

The inter-firm network of the Japanese economy is a dataset that maps out of the entire production-consumpion network of all active firms. It is a snapshot taken in the year 2005, where the nodes are the active firms and the edges joining them show that there is a flow of orders between them. The edges are unweighted but directed from the customer node to the supplier node indicating clearly the direction of money.

Comparing this real world network with the regular lattices investigated in Chapters 4 and 5 highlights how non-rigid actual production-consumpion networks are. Key characteristics are scale-free distributions both for the in- and out-degrees, shallowness in “layers” indicative from the short average path length and ample triangles and cycles [61]. It will shortly be shown that using the generalised directed sandpile model dynamics on the network of the

Japanese economy yields a surprising avalanche-size exponent of approximately $\tau = 1.87$ (Fig 6.1). This is a novel avalanche-size exponent that has not been reported anywhere else. The system qualitatively reproduces the fluctuations in production as observed in the aggregate when the system is critical.

The work presented here is not unique in extending the sandpile model [5] to non-lattice topologies. In fact, this is becoming more feasible with the recent advances of complex systems and networks theory. The BTW model [5] has been investigated on numerous occasions by Goh *et al.* [33, 34, 45, 46] on scale-free undirected networks. A branching process was used to find the avalanche-size exponent τ, which was expressed in terms of the degree exponent γ of scale-free networks. Two distinct regimes were found: for $\gamma > 3$ the avalanche-size exponent was $\tau = 3/2$, which is the same as the classical mean field; and $\tau = \gamma/(\gamma-1)$ for the range $2 < \gamma < 3$. Uncovering two regimes is particularly interesting as one would expect a mean-field exponent only since the branching process enforces heterogeneity and kills correlations.

On small worlds networks, generated from rewiring regular lattices with bidirectional links, the BTW model has also been investigated both with imposed direction [64] and without [21]. Under the directed small world networks, the system is in the mean-field regime regardless of the value of the rewiring probability p. Interestingly though, in the undirected case, there is a sharp cross-over from the classical BTW universality class to the mean-field universality class as the rewiring probability shifts from $p = 0$ to $p > 0$.

Power grids and river streams are just some examples of directed infrastructural networks that are vulnerable to external shocks [57]. The sandpile model is an attractive model for study on complex networks, but the case with imposed direction is still in its infancy. The

avalanche-size exponent of $\tau = 1.87$ has never been observed before and to understand where it comes from one must take a step back to the directed sandpile from the rigid layered lattice, whose behaviour is very well understood and transition step by step to the real world inter-firm network.

6.2 Methods

The generalised directed sandpile dynamics were defined in Section 4.2. Here, these will be used exactly as defined with the only changes being made to the underlying network topologies. In the numerical simulations on lattices, the same lattice sizes as in Chapter 4 were used, where $L = 200, 400, 600$ with constant width $M = 2000$, which meant that $N = 4 \cdot 10^5, 8 \cdot 10^5, 1.2 \cdot 10^6$, respectively. The Japanese inter-firm network was used as given and here $N \approx 10^6$.

As before, in order to eliminate initialisation bias from random initial configurations and let the system reach a steady state a transient period was used: 5×10^5 events for the lattices and 10^6 events for the inter-firm network. More statistics were needed as the networks needed more events to get to a steady state due to the randomness of the structure. For this reason, on the lattices, the whole experiment was repeated on five different realisations of the networks and then averaged to even out any quirks in structure that are not representative of the motifs needed to obtain SOC. Once the systems reached stationarity, the avalanches started being recorded: 10^6 events for the lattices and 10^7 events for the inter-firm network.

The avalanche statistics from the Monte Carlo simulations were analysed using the methods described in Section 4.3 (from page 71), namely by kth moment analysis for extracting the

scaling exponents and logarithmic data binning visualising the avalanche size pdfs.

6.3 Results on less rigid networks

The numerical results are organised as follows: the behaviour of the generalised directed sandpile dynamics on the Japanese inter-firm network are discussed in Section 6.3.1. This naturally leads to an investigation in the dynamics when the underlying structure becomes less rigid.

The first step is to relax the rigidity of the in- and out-degrees by introducing an interlayer distribution, whilst maintaining the strict layer structure. As soon as any heterogeneity is introduced within the layer, be it a Gaussian or scale-free distribution, the system transitions into the mean-field universality class. This modification alone is not enough to reproduce the behaviour observed in the inter-firm network. The results on the lattices with inter-layer distributions but strict layer structure are in Section 6.3.2.

The second step, is to make the network more shallow as is the real-world trade network and create cycles and triangles by relaxing the strict layer constraint. Despite the shallowness of the network, the cycles and triangles should still cause large avalanches to occur since they effectively increase the depth of the system by making an avalanche go back up the lattice and travel downwards again. Adding a small number of long range connections across layers in the direction of travel and against it yields an avalanche-size exponent close to the one found in Japanese inter-firm network. Unfortunately, it is now impossible to perform FSS of the avalanche-size pdfs as the number of layers L is not a characteristic scale of the system. This perturbation is similar to the rewiring done by Watts and Strogatz [93] to

modify a regular lattice into a small-world network. The results on the lattices with long range connections are in Section 6.3.3.

The interlayer distribution and the long range connections are two perturbations to the strictly layered directed sandpile model, that taken together take the system from the classical universality class to the mean field universality class and finally out of the mean-field to produce non-trivial avalanche-size pdf consistent with the behaviour observed on a real-world inter-firm network.

6.3.1 Japanese inter-firm network

The generalised directed sandpile model defined in Section 4.2, can be used to understand fluctuations in the production-consumption network of the economy of a country. A real world network connecting firms in the economy is not strictly layered as the systems investigated thus far, but instead resembles a web of production where links have a direction which may or may not follow the general direction of flow.

The dataset was provided as part of a collaboration with the Research Institute of Economy, Trade and Industry (RIETI) of Japan and has been traditionally collected by Tokyo Shoko Research Ltd. (TSR). The snapshot used here is from the year 2005 and covers the entire production-consumption network of *all* active firms within Japan. The firms are the nodes of the network and the directed links joining them represent money flow from customer nodes to the supplier nodes. The direction of money flow is exactly the same as the direction of orders and hence a direct analogy can be made between the generalised directed sandpile model and inter-firm trade.

The inter-firm trading network consists of approximately one million nodes ($N \approx 10^6$) and four million links. Previous studies of the network structure have shown that this is a typical complex network with a power law degree distribution for both the in- and out- degrees with scale-free exponents $\gamma = 2.35$ and $\gamma = 2.26$, respectively [61, 90, 91], see Eq. (3.1). Other characteristics include a negative degree-degree correlation [90], clear community structures that trace the shape of the economy [40], power laws of money (order) flows [83, 90] and asymmetric behaviour of hubs and authorities [55, 56]. Interestingly, the average path length is only 5.62 and the maximum spanning tree has length 21, which makes this a very shallow network [61].

The nodes in inter-firm network are arranged in a bow-tie structure, meaning that there is a strict in-component (31%) made of the nodes where $k_{i,j}^{in} = 0$, a strict out-component (16%) where nodes have $k_{i,j}^{out} = 0$ and finally a strongly connected component (53%) in between the two that comprises of all the remaining nodes [61]. To implement the generalised directed sandpile dynamics, the in-component will be treated as the top layer where the system will be driven from and will be interpreted as the final retailers in the economy. Similarly, the out-component will be the bottom layer where the final orders of raw materials are made to primary producers. In the strongly connected component is where the avalanches of production will fluctuate and most of the statistics will come from. Finally, all the constraints on inventory, production and sales hold as they were defined in Section 4.2 and are based only on the in-degree $k_{i,j}^{in}$ of each node.

The results of the numerical simulations are displayed in Fig. 6.1. The avalanche-size pdf, in solid black line, has a broad distribution which is consistent with a power-law decay spanning three orders of magnitude. The estimated avalanche-size exponent is $\tau = 1.87$, that is unlike any exponent declared in the two known universality classes: classical two-

dimensional universality class $\tau = 4/3$ (see Section 4.4) and the mean-field universality class $\tau = 3/2$ (see Section 6.3.2), shown in grey dashed lines as guides.

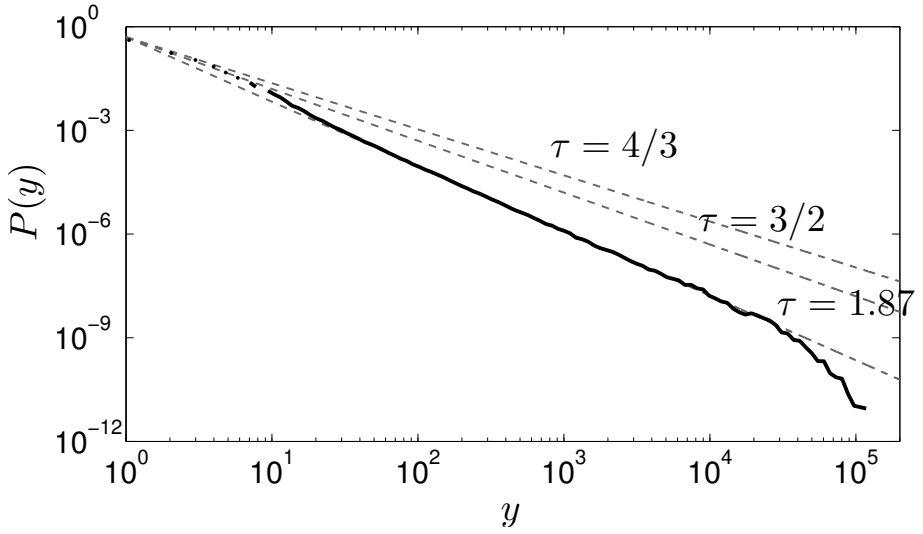


Figure 6.1 **Results on the Japanese inter-firm network.** The avalanche-size pdf $P(y)$ versus the avalanche size y obtained when the directed generalised dynamics evolves on the inter-firm network (solid black line). For more than three orders of magnitude, this pdf is well approximated with a power-law decay $P(y) \propto y^{-1.87}$, for $20 \lesssim y \lesssim 30000$. The grey dashed lines with $\tau = 4/3$ and $\tau = 3/2$ are guides to the eyes for the known universality classes' avalanche-size exponents of directed ($d = 2$) and mean-field, respectively.

6.3.2 Layered lattice with inter-layer distribution of interactions

To get closer to something that resembles the real world inter-firm network avalanche-size exponent observed above one needs to start from the well-understood rigid regular networks described in Chapter 4 and introduce heterogeneity in the in- and out-degrees of the nodes within the layers, whilst keeping the strictly layered structure of the lattice untouched. Different types of inter-layer degree distributions were investigated under the same constraints on inventory, production and sales as introduced in Section 4.2 which are dependent on the in-degree $k^{in}_{i,j}$ of each productive unit.

Gaussian out- and in- degree distribution

The first distribution tested is Gaussian. The out-degree $k_{i,j}^{out}$ of each production node will be Gaussian distributed with $k_{i,j}^{out} \sim \mathcal{N}(\mu, \sigma^2)$ and its suppliers will be chosen randomly (using the Mersenne Twister pseudo-random number generator [52]) from the layer below. Additional constraints on the re-wiring process ensure that the out-degrees $k_{i,j}^{out}$ are greater than two and that each duple of nodes can only have one link connecting them. A distribution was not imposed on the in-degrees $k_{i,j}^{in}$ of the nodes, but due to the CLT, these were Gaussian distributed. In the numerical results displayed in Figure 6.2, the mean coordination number was chosen to be $\mu = 4$ and three different values for the standard deviation $\sigma = 0, 1, 2$ were tested.

The respective scaling exponents were estimated using the moment analysis methods described in Section 4.3 and are reported in Table 6.1. Both scaling exponents τ and D are within error bars of the mean-field universality class for all settings investigated. Note, for the case where $\sigma = 0$ the underlying topology is simply a rewired version of the regular lattice with coordination number $K = 4$ [93].

σ	τ	D	$D(2-\tau)$
0	1.45(5)	1.8(2)	1.00
1	1.47(5)	1.9(2)	1.00
2	1.48(5)	1.9(2)	1.00

Table 6.1 **Scaling exponens on layered lattices with Gaussian out- and in-degree interlayer distributions.** The avalanche-size exponent, τ, and the avalanche-dimension, D, for networks with nodes' out-degrees drawn from a Gausssian distribution with a fixed mean coordination number $\mu = 4$, and standard deviations $\sigma = 0, 1, 2$. Note that the case of $\sigma = 0$ is just a randomly rewired version of the regular lattice with coordination number $K = 4$, see Fig. 6.2 for the data collapse. The numbers in the brackets indicate the estimated errors of the exponents. Within error bars, both scaling exponents are consistent with the mean-field model $\tau = 3/2$ and $D = 2$. The last column shows that the exponents fulfill the scaling relation $D(2-\tau) = 1$, see Eq. (4.11).

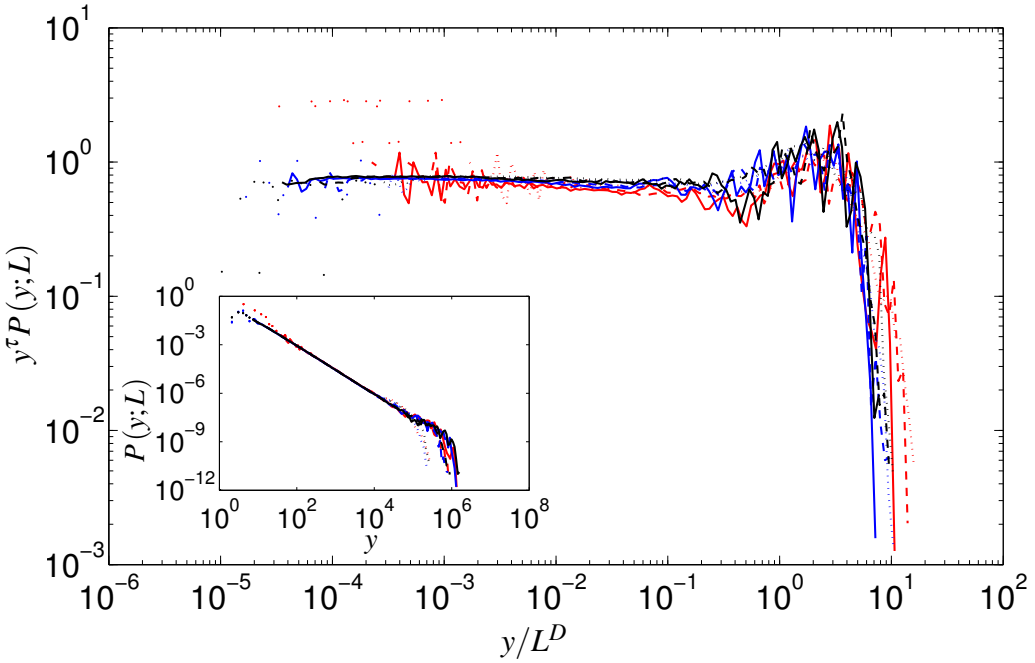


Figure 6.2 **Results on lattices with Gaussian out- and in-degree inter-layer distributions.** The main figure shows the data collapse of the avalanche-size pdfs $P(y;L)$ from networks with underlying Gaussian out-degree distribution, obtained by plotting the transformed avalanche-size pdf $y^\tau P(y;L)$ against the rescaled avalanche size y/L^D using the estimates of the avalanche-size scaling exponents τ and D obtained from moment scaling analysis, see Table 6.1, L=200 (dashed-dotted); L=400 (dashed line); L=600 (solid line). The line colour indicates the standard deviation: $\sigma = 0$ (red), $\sigma = 1$ (blue), $\sigma = 2$ (black). By CLT the in-degree is also Gaussian distributed. The width of the system is $M = 2000$ nodes. The inset displays the avalanche-size pdf $P(y;L)$ versus the avalanche size y.

Scale-free out- and Gaussian in- degree distribution

Secondly, the out-degree $k_{i,j}^{out}$ of each node is drawn from a scale-free distribution with exponent γ: $k_{i,j}^{out} \propto K^{-\gamma}$ for $\gamma = 2.5, 3.0, 3.5$ where $2 \leq k^{out} \leq 20$. In this scenario stubs have been created for all nodes and these are connected to make links. The links are placed randomly between nodes in consecutive layers, ensuring that only one link can ever exist between a pair of nodes. Again, by CLT, the in-degrees $k_{i,j}^{in}$ are Gaussian distributed. The numerical simulation results are displayed in Figure 6.3. As before, the associated scaling exponents were estimated using the moment analysis and are reported in Table 6.2. Both scaling exponents τ and D are within error bars of the mean-field universality class.

γ	τ	D	$D(2-\tau)$
2.5	1.48(5)	1.9(2)	1.00
3.0	1.47(5)	1.9(2)	1.00
3.5	1.46(5)	1.9(2)	1.00

Table 6.2 **Scaling exponents with scale-free out- and Gaussian in-degree inter-layer distributions.** The avalanche-size exponent τ and dimension D for networks with nodes' out-degrees drawn from a truncated scale free distribution with exponent $\gamma = 2.5, 3.0, 3.5$, see Fig. 6.3 for the data collapse. The CLT ensures the distribution of in-degrees is Gaussian. The estimated errors of the exponents are in the brackets. Within error bars, both scaling exponents are consistent with the mean-field model $\tau = 3/2$ and $D = 2$. The last column shows that the exponents fulfill the scaling relation $D(2-\tau) = 1$, see Eq. (4.11).

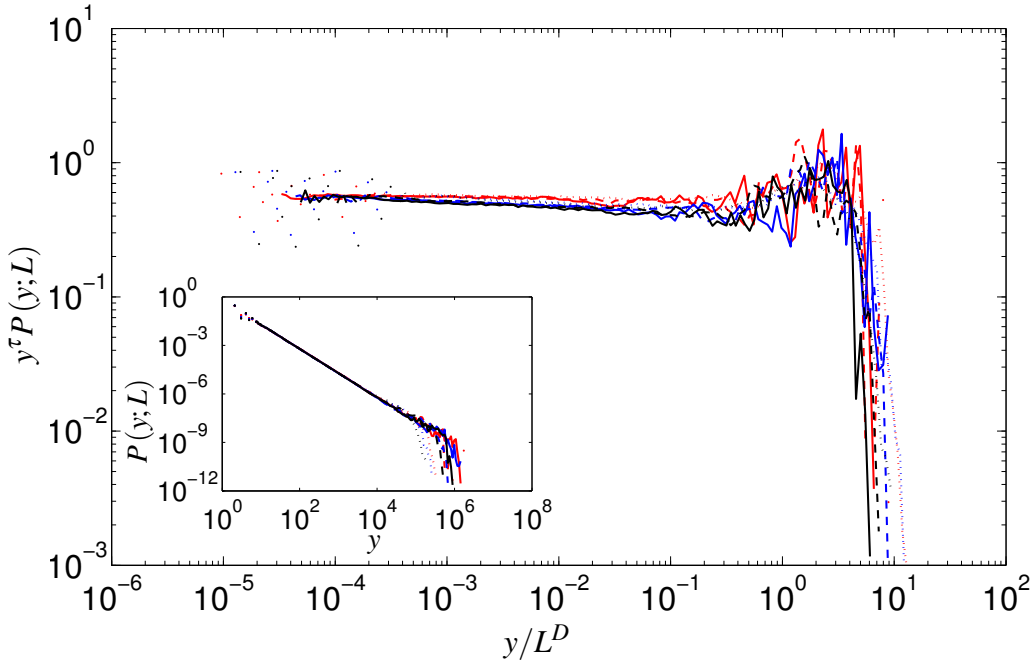


Figure 6.3 **Results on lattices with scale-free out- and Gaussian in-degree inter-layer distributions.** The main figure shows the data collapse of the avalanche-size pdfs $P(y;L)$ from networks with underlying truncated scale-free out-degree distribution and, by Central Limit Theorem (CLT), Gaussian in-degree distribution. These were obtained by plotting the transformed avalanche-size pdf $y^{\tau}P(y;L)$ against the rescaled avalanche size y/L^{D} using the estimates of the avalanche-size scaling exponents τ and D obtained from moment scaling analysis, see Table 6.2. The line style indicates the system size, dashed-dotted: L=200; dashed line: L=400; solid line: L=600. The line colour indicates the scale-free exponent γ: $\gamma = 2.5$ (red), $\gamma = 3.0$ (blue), $\gamma = 3.5$ (black). The width of the system is kept constant at 2000 nodes. The inset displays the avalanche-size pdf $P(y;L)$ plotted against the avalanche size y generated from networks with underlying truncated scale-free out-degree distribution.

Scale-free out- and in- degree distribution

The third distribution used is again scale-free, but in this setting an out-degree distribution is also imposed on the nodes instead of letting things evolve naturally under the CLT. The out-degrees $k_{i,j}^{out}$ of the nodes are scale-free distributed as above with $k_{i,j}^{out} \propto K^{-\gamma}$ for $\gamma = 2.5, 3.5$ and $2 \leq k^{out} \leq 20$. The out-degrees $k_{i,j}^{out}$ of layer t were then re-shuffled and assigned as the in-degrees $k_{i,j}^{in}$ of nodes in the layer below $t+1$. The stubs were then connected to create links between adjacent layers, whilst avoiding multiple links between nodes. The numerical results are displayed in Figure 6.4. As above, the associated scaling exponents were estimated using the moment analysis and are reported in Table 6.3. Both scaling exponents $\tau = 3/2$ and $D = 2$ are within error bars of the mean-field universality class in all settings tested. Note, that in the setting where the degree distribution exponent $\gamma = 2.5$, the avalanche-size exponent found is very different to the one predicted by the branching process of Goh *et al.* $\tau = 5/3$ [33].

γ	τ	D	$D(2-\tau)$
2.5	1.50(5)	2.0(2)	1.01
3.5	1.48(5)	1.9(2)	1.00

Table 6.3 **Scaling exponents on layered lattices with scale-free in- and out-degree inter-layer distributions.**The avalanche-size exponent, τ, and the avalanche-dimension, D, for networks with nodes' in- and out-degrees were both drawn from a truncated scale free distribution with exponents $\gamma = 2.5, 3.5$, see Fig. 6.4 for the data collapse. The numbers in the brackets indicate the estimated errors of the exponents. Within error bars, both scaling exponents are consistent with the mean field-model $\tau = 3/2$ and $D = 2$. The last column shows that the exponents fulfill the scaling relation $D(2-\tau) = 1$, see Eq. (4.11).

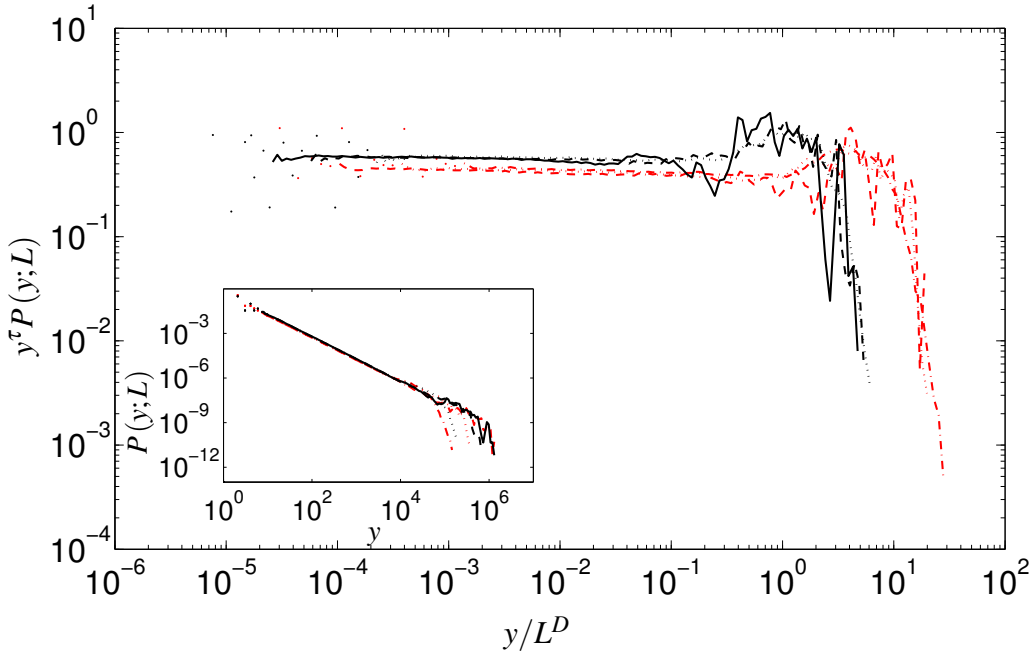


Figure 6.4 **Results on lattices with scale-free in- and out-degree inter-layer distributions.** The main figure shows the data collapse of the avalanche-size pdfs $P(y;L)$ from networks with underlying truncated scale-free in- and out-degree distribution. These were obtained by plotting the transformed avalanche-size pdf $y^{\tau}P(y;L)$ against the rescaled avalanche size y/L^{D} using the estimates of the avalanche-size scaling exponents τ and D obtained from moment scaling analysis, see Table 6.3. The line style indicates the system size, dashed-dotted: L=100; dotted line: L=200; dashed line: L=400; solid line: L=600. The line colour indicates the scale-free exponent γ: $\gamma = 2.5$ (red) with $L = 100, 200, 400$ and $\gamma = 3.5$ (black) with $L = 200, 400, 600$. The width of the system is $M = 2000$ nodes. The inset displays the avalanche-size pdf $P(y;L)$ versus the avalanche size y.

6.3.3 Long range connections across layers

It is clear from the results in Section 6.3.2 that any perturbation to the underlying rigid lattice that maintains that strict layer component, puts the system into the mean field universality class with critical exponents $\tau = 3/2$ and $D = 2$. This is nowhere near the avalanche-size exponent $\tau = 1.87$ observed when the directed sandpile model is let to evolve on the Japanese inter-firm network, see Fig. 6.1. One might ask what other characteristics of inter-firm network can one bring onto the underlaying topologies studied thus far?

The Japanese inter-firm network has an evident direction of flow in the in- and out- components but it does not have a unique direction in the strongly connected component, as the economy naturally evolved in a non strictly layered manner. In fact, one of the most surprising characteristics of this network, the small average path length of 5.62 [61], is due to non-strict layer structure, the lack of unique direction and also the giant hubs created from the scale-free degree distributions. These characteristics motivate a change from the strictly layered lattices to lattice structures that are shallower and with cycles that might make large avalanches possible.

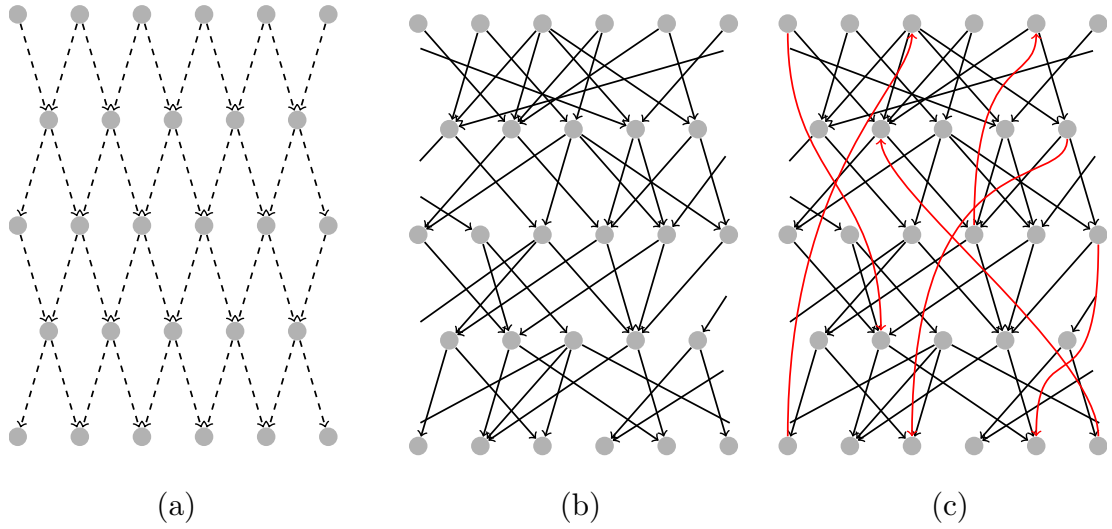


Figure 6.5 **Illustration of the types of layered topologies tested.** Networks shown are subsets of (a) two-dimensional rigid regular directed lattice with coordination number $K = 2$ (black dashed lines); (b) layered network with a randomised inter-layer degree distribution (e.g. Gaussian or Scale-free) with randomly chosen neighbours in the adjacent layer below (black solid lines); (c) networks created by adding links connecting non adjacent layers (red solid lines) in both directions to the layered network with randomised degree distribution (black solid lines). In all cases, periodic boundary conditions are applied to the left- and right-most nodes to form a cylindrical structure.

The layered network from the ones tested above that most resembles the scale-free distributions on the inter-firm network is the one with both in- and out-degrees scale-free distributed. This is chosen as the base network and an attempt is made to disrupt some of the strict layer structure. A small proportion of long range connections in an otherwise layered network is added, some in the direction of the flow and some against it, as shown in the illustration Fig. 6.5. This simple modification reduced the average path length of the lattice and created triangles and cycles in the network, much like the key characteristics observed on the Japanese inter-firm network. The top layer is now the in-component since all its nodes have zero in-degree $k_{i,j}^{in} = 0$ and the bottom layer is the out-component where the nodes have zero out-degree $k_{i,j}^{out} = 0$. The layers in between play the part of the strongly connected component, although this was not a condition that was imposed here.

The long range connections were implemented with a random probability p_{lr}, where for each node a random number was generated and if this was within 0 and p_{lr} then one of its links would be randomly rewired to another node in the network which was not in the adjacent layer. Different p_{lr} values were tested ($p_{lr} \in [0.05, 0.10, 0.25, 0.50, 0.75]$) and for all values the system steps out of the mean field and produces non-trivial avalanche behaviour.

The case where $p_{lr} = 0.25$ is displayed in Fig. 6.6 as it is the closest one that qualitatively reproduces the avalanche-size pdf of the Japanese inter-firm network. In this network, the average path length was reduced from 114 to 12 with the introduction of the long range links, which at first glance may not seem like a drastic change, but upon closer inspection the perturbation brought the average path length to the same order of magnitude as the inter-firm network (5.62). Large avalanches are impossible in a shallow network with strict layer structure, but with the addition of long range links these become possible as seen in the non-trivial avalanche-size pdf.

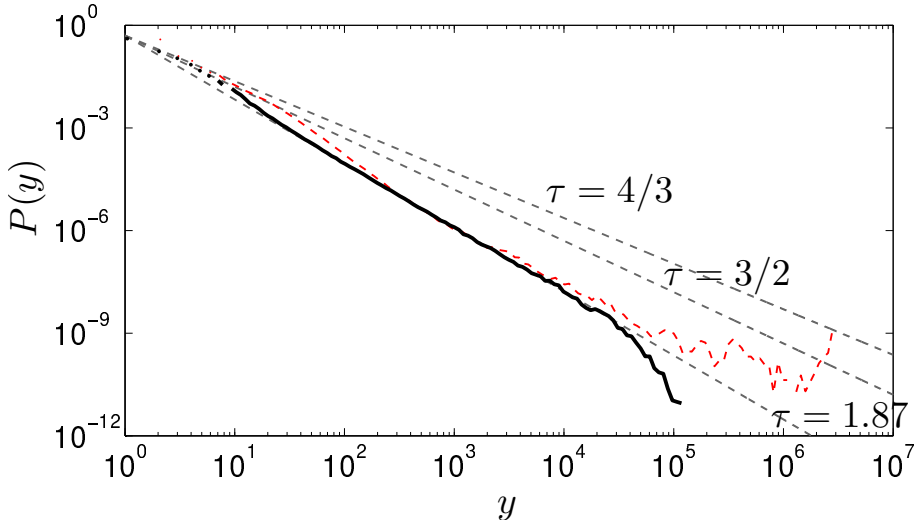


Figure 6.6 **Results on lattices with long-range connections.** The avalanche-size pdf $P(y)$ versus the avalanche-size y obtained using the inter-firm Japanese network (solid black line). The dashed red line is the pdf $P(y)$ obtained with 25% of long range connections across layers in an otherwise layered network with nodes in- and out- degree drawn from a truncated scale-free distribution with exponent $\gamma = 2.5$ and system size $L = 400$. The grey dashed lines are guides to the eyes for the different avalanche-size exponents ($\tau = 4/3$ and $3/2$) of the known universality classes for the directed sandpile model and the approximate $\tau = 1.87$ that seems to fit the pdfs of inter-firm Japanese network.

6.4 Summary

The generalised directed sandpile model is a deterministic model whose dynamics can be used to investigate fluctuations in the behaviour of socio-economic systems. Moving away from the strict layer structure and allowing the in- and out- degrees of the node to be drawn from Gaussian and/or scale-free distributions showed that, regardless of the underlying topology, any slight perturbation takes the system out of the classical two-dimensional directed sandpile model universality class with $\tau = 4/3$ and $D = 3/2$ and into the mean field universality class with $\tau = 3/2$ and $D = 2$ [26].

Letting the dynamics evolve on a directed, complex but non-layered network, the inter-firm trade network of all active firms in Japan yields a novel avalanche-size exponent $\tau = 1.87$, which is beyond the two well known ones. The new exponent is steeper than both the two-dimensional directed sandpile model and the mean-field: $1.87 > 3/2 > 4/3$. When $\tau = 4/3$ there are clear spacial correlations in the underlying topology but any randomness in the inter-layer structure breaks these correlations and yields $\tau = 3/2$. Having an exponent steeper than the mean-field suggests that there is something beyond the correlations that may be the cause. It is rare to find an avalanche-size exponent beyond the mean-field one in sandpile models [72].

Adding a small proportion of randomly placed long-range connections to an otherwise layered network with scale-free inter-layer distributions produces a non-trivial avalanche-size pdf. This modification tries to mimic some characteristics found in the inter-firm network by destroying the strict layer structure, shortening the average path length, introducing cycles and triangles in the system but not imposing a strongly connected component. The avalanche-size pdfs are qualitatively close to the ones observed when the generalised sandpile model dynamics evolves on the Japanese inter-firm network. However, no scaling is present, which implies that something is missing and that perhaps other structural modifications are needed. Finite-size scaling (see Section 4.3) cannot be performed here as the system size that is needed for this is no longer the lattice size; the long-range connections caused heterogeneity in the underlying network and therefore the effective system size is no longer well defined.

There is a strong case here that a new universality class may exist for the directed sandpile model on lattices beyond the two well known ones. If so, then a strongly connected component is an essential ingredient for this. Key components of the strongly connected

component were mimicked on lattice structures using a combination of an inter-layer distributions and a small proportion of long-range links across layers, as these two taken together created behaviour that qualitatively resembled the one found on a real human engineered socio-economic network.

It is of great scientific interest to determine whether such a new universality class actually exists and moreover to identify the exact structural properties that cause self organised criticality to emerge as this is detrimental to the socio-economic system.

Chapter 7

Discussion

7.1 Conclusions

Several conclusions can be drawn from this research as well as leads for further investigation.

There exist many different universality classes for sandpile models with slight variations in dynamics, many of which are well documented [72]. For example, the universality classes of the stochastic Manna model [51] have been thoroughly explored on directed lattices [43, 62, 66, 67]. Despite this, when generalising the deterministic BTW [5] dynamics and investigating its behaviour on strictly layered and directed networks only two universality classes are observed: the classical two-dimensional directed sandpile model universality class with $\tau = 4/3$ and $D = 3/2$ (see Chapter 4) on regular lattices with coordination number $K \geq 2$, and the mean-field universality class, with $\tau = 3/2$ and $D = 2$ (see Chapter 6)

as soon as an inter-layer distribution of the in- and out-degrees is introduced by simply rewiring some links within layers.

On regular lattices, as the coordination number increases from $K = 2$ to $K > 2$, the scaling exponents τ and D seem to drift slightly from the two-dimensional directed sandpile model universality class with $\tau = 4/3$ and $D = 3/2$ (see Table 4.1). A hypothesis was made that the apparent drift is due to finite-size effects and this was investigated both analytically and numerically (see Chapter 5). It was proven analytically for $K = 3$ on a strictly layered regular lattice that the system is still in the two-dimensional directed sandpile model universality class. Furthermore, taking corrections to scaling into account, see Eq. (5.52), data from large scale numerical simulations for $K = 3$ and 4 are consistent with these systems being in the same universality class, see Table 5.1.

The existence of only two universality classes is fairly intuitive if one considers the structure of the underlying networks. The strictly layered, regular lattices have extremely constrained structures that create correlations in the activity of the dynamics. However, these correlations in activity are destroyed the moment any randomisation is introduced within the layers that interrupts the rigid, regular lattice structure. This becomes abundantly clear when one compares the result obtained from the setup of the regular lattice with coordination number $K = 4$ with the one obtained from the network with the out-degrees of nodes drawn from a Gaussian distribution $k_{i,j}^{out} \sim \mathcal{N}(4,0)$. Even though the latter lattice structure is simply a rewired version of the former regular lattice and all nodes have exactly four neighbours in each adjacent layer, but now randomly connected, the two systems belong to distinct universality classes: the classical two-dimensional directed sandpile model universality class on the regular lattice where $K = 4$ (see Table 4.1); and and the mean-field universality class with $\tau = 3/2$ and $D = 2$ for the Gaussian inter-layer distributed lattice (see Table 6.1). There

seems to be an abrupt transition between the two universality classes, which is induced by the breaking of the correlation in activity. This behaviour was evident in all tested inter-layer distributions (see Tables 6.2 and 6.3).

When the generalised sandpile model dynamics is let to evolve on a complex direct yet non-layered real-world network (the Japanese inter-firm network), a surprising behaviour is observed: a novel non-trivial avalanche-size exponent of $\tau = 1.87$ emerges, see Fig. 6.6. This exponent falls outside both of the two known universality classes ($1.87 > 3/2 > 4/3$) and is even steeper than the mean-field, a very rare occurrence in sandpile models [72], implying that there is something beyond breaking the correlations that comes into play here. A clue is given when looking at the underlying structure of this real-world network.

The Japanese inter-firm network, on which novel non-trivial avalanche-size exponent was observed, is a shallow network with the typical bow-tie structure of a real-world directed network, with a strongly connected component that is not layered but instead has cycles, triangles and other network motifs [61]. Imposing these characteristics on the rewired lattices by simply adding a small proportion of random long-range connections between non-adjacent layers and in doing so destroying the strict layer structure of the system, yields a non-trivial avalanche-size pdf; this is qualitatively similar to the one observed on the inter-firm network, but not a perfect match suggesting that additional structural constraints need to be imposed. Unfortunately, FSS cannot be performed since the long-range connections induce structural heterogeneity in the system and what was before a well-defined system size that could be used in the FSS calculations is now a very ambiguous and ill-defined quantity.

However, these facts considered together lead us boldly to hypothesise that a new universal-

ity class exists for the generalised directed sandpile model and moreover, that the structure of the underlying network is crucial, particularly the long-range connections that were initially only introduced as a means for the system to sustain large avalanches.

7.2 Outlook

This thesis only scratches the surface of what is needed to quantitatively prove that in fact a new universality class exists. Investigating this further is of great scientific interest as, from what was observed thus far, the underlying structure that gives rise to this behaviour is found in abundance in human engineered networks.

Characterisation of complex networks is a rapidly developing field of research [20] that is increasingly becoming more applicable to many areas of research, from neuroscience [47, 65] to computational chemistry [13, 22, 44] and finance [61], to mention but a few. All the detailed structural properties that enable SOC to exist in these complex networks need to be identified and understood; a system in a self-organised critical state produces unpredictable large events that can be detrimental to its survivability and sustainability.

Economies, for example, are by nature complex socio-economic systems whose aggregate activity is not always well understood. Large shocks in economic activity, though rare, are very destructive. This research shows that these large events are directly enabled by the underlying production-consumption network between firms in the economy. In the sandpile model, the fluctuations are predictable but in real life, since you do not have complete information about the system, they cannot be predicted at all or you have to rely on other analytical tools to monitor the evolution of key observables in the system [70]. The unpre-

dictability of the fluctuations is very costly and detrimental to society and thus it is highly desirable to prevent, or at least mitigate the emerging shocks. Therefore, it would be very interesting to investigate whether these large scale fluctuations can be prevented or if the system simply adapts to any intervention such that they would persist.

A complexity and networks approach can be taken to uncover the mechanisms in place that make socio-economic systems in nature sustainable and the lessons learned can be incorporated in human engineered systems. Sustainability is a key issue of the 21^{st} century and as planetary engineers the weight falls on our shoulders.

Bibliography

[1] W Ross Ashby. An introduction to cybernetics. 1957.

[2] Per Bak. How Nature Works: The Science of Self Organized Criticality Springer Verlag. *New York*, 1996.

[3] Per Bak and Kim Sneppen. Punctuated equilibrium and criticality in a simple model of evolution. *Physical review letters*, 71(24):4083, 1993.

[4] Per Bak and Chao Tang. Earthquakes as a selforganized critical phenomenon. *Journal of Geophysical Research: Solid Earth (1978–2012)*, 94(B11):15635–15637, 1989.

[5] Per Bak, Chao Tang, and Kurt Wiesenfeld. Self-organized criticality: An explanation of the 1/f noise. *Physical review letters*, 59(4):381, 1987.

[6] Per Bak, Chao Tang, and Kurt Wiesenfeld. Self-organized criticality. *Physical review A*, 38(1):364, 1988.

[7] Per Bak, Kan Chen, José Scheinkman, and Michael Woodford. Aggregate fluctuations from independent sectoral shocks: self-organized criticality in a model of production and inventory dynamics. *Ricerche Economiche*, 47(1):3–30, 1993.

[8] Per Bak, Kim Christensen, Leon Danon, and Tim Scanlon. Unified scaling law for earthquakes. *Physical review letters*, 88(17):178501, 2002.

[9] Stafford Beer. *Brain of the firm: the managerial cybernetics of organization*. J. Wiley New York, 1981.

[10] Javier Borondo, Florentino Borondo, Carlos Rodriguez-Sickert, and Cesar A Hidalgo. To each according to its degree: The meritocracy and topocracy of embedded markets. *Scientific reports*, 4, 2014.

[11] Gru Brundtland, Mansour Khalid, Susanna Agnelli, Sali Al-Athel, Bernard Chidzero, Lamina Fadika, Volker Hauff, Istvan Lang, Ma Shijun, Margarita Morino de Botero, et al. Our common future ("brundtland report"). 1987.

[12] Mark Buchanan. *Nexus: small worlds and the groundbreaking theory of networks*. WW Norton & Company, 2003.

[13] Shujuan Cao, Matthias Dehmer, and Yongtang Shi. Extremality of degree-based graph entropies. *Information Sciences*, 278:22–33, 2014.

[14] Vasco M Carvalho. *Aggregate fluctuations and the network structure of intersectoral trade*. ProQuest, 2008.

[15] Nicholas A Christakis and James H Fowler. *Connected: The amazing power of social networks and how they shape our lives*. Harper Press, 2010.

[16] Kim Christensen and Nicholas R Moloney. *Complexity and criticality*, volume 1. Imperial College Press, 2005. ISBN 186094504X.

[17] Kim Christensen, Nadia Farid, Gunnar Pruessner, and Matthew Stapleton. On the scaling of probability density functions with apparent power-law exponents less than unity. *The European Physical Journal B*, 62(3):331–336, 2008.

[18] Kim Christensen, Dario Papavassiliou, Alexandre de Figueiredo, Nigel R Franks, and Ana B Sendova-Franks. Universality in ant behaviour. *Journal of The Royal Society Interface*, 12(102):20140985, 2015.

[19] "complexity". *Oxford dictionary of English*. Oxford University Press, 2010.

[20] L da F Costa, Francisco A Rodrigues, Gonzalo Travieso, and Paulino Ribeiro Villas Boas. Characterization of complex networks: A survey of measurements. *Advances in Physics*, 56(1):167–242, 2007.

[21] L De Arcangelis and H J Herrmann. Self-organized criticality on small world networks. *Physica A: Statistical Mechanics and its Applications*, 308(1):545–549, 2002.

[22] Matthias Dehmer and Martin Grabner. The discrimination power of molecular identification numbers revisited. *MATCH Commun. Math. Com put. Chem*, 69(3):785–794, 2013.

[23] René Descartes. A discourse of a method for the well guiding of reason and the discovery of truth in the sciences. 1937.

[24] Deepak Dhar. The abelian sandpile and related models. *Physica A: Statistical Mechanics and its Applications*, 263(1):4–25, 1999.

[25] Deepak Dhar. Theoretical studies of self-organized criticality. *Physica A: Statistical Mechanics and its Applications*, 369(1):29–70, 2006.

[26] Deepak Dhar and Ramakrishna Ramaswamy. Exactly solved model of self-organized critical phenomena. *Physical review letters*, 63(16):1659, 1989.

[27] Deepak Dhar, Gunnar Pruessner, Paul Expert, Kim Christensen, and Nicky Zachariou. Directed abelian sandpile with multiple downward neighbors. *Phys. Rev. E*, 93: 042107, Apr 2016. doi: 10.1103/PhysRevE.93.042107. URL http://link.aps.org/doi/10.1103/PhysRevE.93.042107.

[28] Simon Dresner. *The principles of sustainability*. Earthscan, 2008.

[29] Angela Espinosa and Jon Walker. *A complexity approach to sustainability: theory and application*, volume 1. World Scientific, 2011.

[30] Food and Agriculture Organization of the United Nations. *1.02 billion people hungry*. [Online]. Available from: http://www.fao.org/news/story/en/item/20568/icode/. [Accessed 13th February 2016].

[31] Nigel R. Franks. Army ants: A collective intelligence: A neural network seems an apt analogy as a colony of army ants navigates the tropical rain forest. *American Scientist*, 77(2):138–145, 1989. ISSN 00030996. URL http://www.jstor.org/stable/27855654.

[32] World Wildlife Fund. *World conservation strategy: Living resource conservation for sustainable development*. Gland, Switzerland: IUCN, 1980.

[33] K-I Goh, D-S Lee, B Kahng, and D Kim. Sandpile on scale-free networks. *Physical review letters*, 91(14):148701, 2003.

[34] K-I Goh, D-S Lee, B Kahng, and D Kim. Cascading toppling dynamics on scale-free networks. *Physica A: Statistical Mechanics and its Applications*, 346(1):93–103, 2005.

[35] Deborah M Gordon. *Ant encounters: interaction networks and colony behavior*. Princeton University Press, 2010.

[36] Mark Granovetter. Economic action and social structure: The problem of embeddedness. *American journal of sociology*, pages 481–510, 1985.

[37] Graham Harris. *Seeking sustainability in an age of complexity*. Cambridge University Press, 2007.

[38] Masaaki Hirooka. Nonlinear dynamism of innovation and business cycles. *Journal of evolutionary economics*, 13(5):549–576, 2003.

[39] Bert Hölldobler and Edward O Wilson. Journey to the ants: a story of scientific exploration. 1998.

[40] T Iino, K Kamehama, H Iyetomi, Y Ikeda, T Ohnishi, H Takayasu, and M Takayasu. Community structure in a large-scale transaction network and visualization. In *Journal of Physics: Conference Series*, volume 221, page 012012. IOP Publishing, 2010.

[41] Henrik Jeldtoft Jensen. *Self-organized criticality: emergent complex behavior in physical and biological systems*, volume 10. Cambridge University Press, 1998. ISBN 0521483719.

[42] Leo P Kadanoff, Sidney R Nagel, Lei Wu, and Su-min Zhou. Scaling and universality in avalanches. *Physical Review A*, 39(12):6524, 1989.

[43] Morten Kloster, Sergei Maslov, and Chao Tang. Exact solution of a stochastic directed sandpile model. *Physical Review E*, 63(2):26111, 2001.

[44] Veronika Kraus, Matthias Dehmer, and Michael Schutte. On sphere-regular graphs and the extremality of information-theoretic network measures. *MATCH Commun. Math. Comput. Chem*, 70(3):885–900, 2013.

[45] D S Lee, K I Goh, B Kahng, and D Kim. Branching process approach to avalanche dynamics on complex networks. *JOURNAL-KOREAN PHYSICAL SOCIETY*, 44(1): 633–637, 2004.

[46] D-S Lee, K-I Goh, B Kahng, and Daeho Kim. Sandpile avalanche dynamics on scale-free networks. *Physica A: Statistical Mechanics and its Applications*, 338(1):84–91, 2004.

[47] Louis-David Lord, Paul Allen, Paul Expert, Oliver Howes, Matthew Broome, Renaud Lambiotte, Paolo Fusar-Poli, Isabel Valli, Philip McGuire, and Federico E Turkheimer. Functional brain networks before the onset of psychosis: a prospective fMRI study with graph theoretical analysis. *NeuroImage: Clinical*, 1(1):91–98, 2012.

[48] James Lovelock. *Gaia: A new look at life on earth*. Oxford University Press, 2000.

[49] James Lovelock. *The ages of Gaia: A biography of our living earth*. Oxford University Press, USA, 2000.

[50] S Lübeck. Logarithmic corrections of the avalanche distributions of sandpile models at the upper critical dimension. *Physical Review E*, 58(3):2957, 1998.

[51] S S Manna, A D Chakrabarti, and R Cafiero. Critical states in a dissipative sandpile model. *Physical Review E*, 60(5):R5005, 1999.

[52] Makoto Matsumoto and Takuji Nishimura. Mersenne twister: a 623-dimensionally equidistributed uniform pseudo-random number generator. *ACM Transactions on Modeling and Computer Simulation (TOMACS)*, 8(1):3–30, 1998.

[53] Donella H Meadows and Diana Wright. *Thinking in systems: A primer*. chelsea green publishing, 2008.

[54] Melanie Mitchell. *Complexity: A guided tour*. Oxford University Press, 2009.

[55] W Miura, H Takayasu, and M Takayasu. The origin of asymmetric behavior of money flow in the business firm network. *The European Physical Journal-Special Topics*, 212 (1):65–75, 2012.

[56] Wataru Miura, Hideki Takayasu, and Misako Takayasu. Effect of coagulation of nodes in an evolving complex network. *Physical review letters*, 108(16):168701, 2012.

[57] Enys Mones, Nuno AM Araújo, Tamás Vicsek, and Hans J Herrmann. Shock waves on complex networks. *Scientific reports*, 4, 2014.

[58] J. Simmons M. Mogie N. R. Franks, A. B. Sendova-Franks. Convergent evolution, superefficient teams and tempo in old and new world army ants. *Proceedings: Biological Sciences*, 266(1429):1697–1701, 1999. ISSN 09628452. URL http://www.jstor.org/stable/51526.

[59] Mark Newman. *Networks: an introduction*. Oxford university press, 2010.

[60] Jon Norberg and Graeme S Cumming. *Complexity theory for a sustainable future*. Columbia University Press, 2013.

[61] Takaaki Ohnishi, Hideki Takayasu, and Misako Takayasu. Hubs and authorities on Japanese inter-firm network: Characterization of nodes in very large directed networks. *Progress of Theoretical Physics Supplement*, 179:157–166, 2009.

[62] Maya Paczuski and Kevin E Bassler. Theoretical results for sandpile models of self-organized criticality with multiple topplings. *Physical Review E*, 62(4):5347, 2000.

[63] Maya Paczuski and Kevin E Bassler. Theoretical results for sandpile models of self-organized criticality with multiple topplings. *Physical Review E*, 62(4):5347, 2000.

[64] Gui-Jun Pan, Duan-Ming Zhang, Yan-Ping Yin, and Min-Hua He. Sandpile on directed small-world networks. *Physica A: Statistical Mechanics and its Applications*, 383(2): 435–442, 2007.

[65] Anand S Pandit, Paul Expert, Renaud Lambiotte, Valerie Bonnelle, Robert Leech, Federico E Turkheimer, and David J Sharp. Traumatic brain injury impairs small-world topology. *Neurology*, 80(20):1826–1833, 2013.

[66] Romualdo Pastor-Satorras and Alessandro Vespignani. Universality classes in directed sandpile models. *Journal of Physics A: Mathematical and General*, 33(3):L33, 2000.

[67] Romualdo Pastor-Satorras and Alessandro Vespignani. Critical behavior and conservation in directed sandpiles. *Physical Review E*, 62(5):6195, 2000.

[68] Ole Peters, Christopher Hertlein, and Kim Christensen. A complexity view of rainfall. *Physical review letters*, 88(1):18701, 2001.

[69] Suani TR Pinho and Roberto FS Andrade. An abelian model for rainfall. *Physica A: Statistical Mechanics and its Applications*, 255(3):483–495, 1998.

[70] Duccio Piovani, Jelena Grujic, and Henrik Jeldtoft Jensen. Forecasting systemic transitions in high dimensional stochastic complex systems. In *Journal of Physics: Conference Series*, volume 633, page 012001. IOP Publishing, 2015.

[71] William H Press, Saul A Teukolsky, William T Vetterling, and Brian P Flannery. *Numerical Recipes in C, 2nd Ed.*, volume 2. Cambridge University Press.

[72] Gunnar Pruessner. *Self-organised criticality: theory, models and characterisation*. Cambridge University Press, 2012. ISBN 0521853354.

[73] CJ Rhodes and P Jones. Inferring missing links in partially observed social networks. *Journal of the operational research society*, 60(10):1373–1383, 2009.

[74] CJ Rhodes and EMJ Keefe. Social network topology: a bayesian approach. *Journal of the operational research society*, 58(12):1605–1611, 2007.

[75] Thomas O Richardson, Elva JH Robinson, Kim Christensen, Henrik J Jensen, Nigel R Franks, and Ana B Sendova-Franks. Record dynamics in ants. *PLoS one*, 5(3):e9621, 2010.

[76] Thomas Owen Richardson, Kim Christensen, Nigel Rigby Franks, Henrik Jeldtoft Jensen, and Ana Blagovestova Sendova-Franks. Ants in a labyrinth: a statistical mechanics approach to the division of labour. *PLoS One*, 6(4):e18416, 2011.

[77] Jose A Scheinkman and Michael Woodford. Self-organized criticality and economic fluctuations. *The American Economic Review*, pages 417–421, 1994.

[78] Friedrich Schmidt-Bleek. *The earth: natural resources and human intervention*. Haus Publishing, 2009.

[79] Beer Stafford. Platform for change. *New York: John Wile and Sons*, 1975.

[80] Will Steffen, Meinrat O Andreae, Bert Bolin, Peter M Cox, Paul J Crutzen, Ulrich Cubasch, Hemuznn Held, Nebojia Nakidenovic, Robert J Scholes, Liana Talaue-McManus, et al. Abrupt changes: the achilles' heels of the earth system. *Environment: Science and Policy for Sustainable Development*, 46(3):8–20, 2004.

[81] Will Steffen, Regina Angelina Sanderson, Peter D Tyson, Jill Jäger, Pamela A Matson, Berrien Moore III, Frank Oldfield, Katherine Richardson, Hans Joachim Schellnhuber, Billie L Turner, et al. *Global change and the earth system: a planet under pressure*. Springer Science & Business Media, 2004.

[82] Bela Suki, Albert-Laszlo Barabasi, Zoltán Hantos, Ferenc Peták, and H Eugene Stanley. Avalanches and power-law behaviour in lung inflation. *Nature*, 368(6472):615–618, 1994.

[83] Koutarou Tamura, Wataru Miura, Misako Takayasu, Hideki Takayasu, Satoshi Kitajima, and Hayato Goto. Estimation of flux between interacting nodes on huge interfirm networks. In *International Journal of Modern Physics: Conference Series*, volume 16, pages 93–104. World Scientific, 2012.

[84] Richard J Trudeau. *Introduction to graph theory*. Dover Publications, 1993.

[85] United Nations. *United Nations Conference on Environment and Development (UNCED or the Earth Summit)*. [Online]. Available from: https://web.archive.org/web/20120121185811/http://www.un.org/geninfo/bp/enviro.html, . [Accessed 13th February 2016].

[86] United Nations. *United Nations Millenium Goals*. [Online]. Available from: http://www.un.org/millenniumgoals/bkgd.shtml, . [Accessed 31st January 2016].

[87] United Nations Development Programme. *Kyoto Protocol to the United Nations Framework Convention on Climate Change*. [Online]. Available from: http://unfccc.int/resource/docs/convkp/kpeng.pdf. [Accessed 13th February 2016].

[88] United Nations Educational, Scientific and Cultural Organization (UNESCO). *EFA Global Monitoring Report 2010, Reaching the marginalized*. [Online]. Available from: http://unesdoc.unesco.org/images/0018/001866/186606E.pdf. [Accessed 13th February 2016].

[89] Pável Vázquez, A Jesús, Karla G Cedano, Manuel Martínez, and Henrik J Jensen. An entangled model for sustainability indicators. *PloS one*, 10(8):e0135250, 2015.

[90] Hayafumi Watanabe. Mean field approximation for biased diffusion on japanese interfirm trading network. *PloS one*, 9(3):e91704, 2014.

[91] Hayafumi Watanabe, Hideki Takayasu, and Misako Takayasu. Biased diffusion on the japanese inter-firm trading network: estimation of sales from the network structure. *New Journal of Physics*, 14(4):043034, 2012.

[92] Duncan J Watts. *Six degrees: The science of a connected age*. Vintage Books, 2004.

[93] Duncan J Watts and Steven H Strogatz. Collective dynamics of 'small-world'networks. *Nature*, 393(6684):440–442, 1998.

[94] WCC. *Report of ecumenical study conference on science and technology for human development.* Geneva: World Council of Churches, 1974.

[95] Klaus Wiegandt. *Our Planet: How Much More Can Earth Take?* Haus Pub, 2008.

[96] Norbert Wiener. *Cybernetics or Control and Communication in the Animal and the Machine*, volume 25. MIT press, 1961.

[97] Uffe Kock Wiil, Jolanta Gniadek, and Nasrullah Memon. Measuring link importance in terrorist networks. In *Advances in Social Networks Analysis and Mining (ASONAM), 2010 International Conference on*, pages 225–232. IEEE, 2010.

[98] Nicky Zachariou, Paul Expert, Misako Takayasu, and Kim Christensen. Generalised Sandpile Dynamics on Artificial and Real-World Directed Networks. *PLoS ONE*, 10 (11):e0142685, 2015. doi: 10.1371/journal.pone.0142685. URL http://dx.doi.org/10.1371%2Fjournal.pone.0142685.